AEDC-TR-95-8

TECHNICAL REPORTS
FILE COPY

OCT 2 8 1996

Demonstrations of a
Pressure Sensitive Paint Data System
in the AEDC Propulsion Wind Tunnel 16T

M. E. Sellers
Micro Craft Technology/AEDC Operations

October 1995

Final Report for Period October 1993 — October 1994

ARNOLD ENGINEERING DEVELOPMENT CENTER
ARNOLD AIR FORCE BASE, TENNESSEE
AIR FORCE MATERIEL COMMAND
UNITED STATES AIR FORCE

This report has been reviewed by the Office of Public Affairs (PA) and is releasable to the National Technical Information Service (NTIS). At NTIS, it will be available to the general public, including foreign nations.
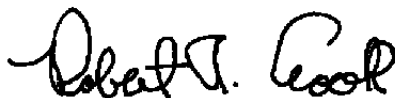
APPROVAL STATEMENT

This report has been reviewed and approved.

J. A. COSSENTINE, CAPT, USAF
Project Manager Applied Technology Division
Operations Directorate

Approved for publication:

FOR THE COMMANDER

ROBERT T. CROOK
Chief, Applied Technology Division
Operations Directorate

REPORT DOCUMENTATION PAGE

Public reporting burden for this collection of information is estimated to average 1 hour per response, including the time for reviewing instructions, searching existing data sources, gathering and maintaining the data needed, and completing and reviewing the collection of information. Send comments regarding this burden estimate or any other aspect of this collection of information, including suggestions for reducing this burden, to Washington Headquarters Services, Directorate for Information Operations and Reports, 1215 Jefferson Davis Highway, Suite 1204, Arlington, VA 22202-4302, and to the Office of Management and Budget, Paperwork Reduction Project (0704-0188), Washington, DC 20503

1 AGENCY USE ONLY (Leave blank)	2 REPORT DATE	3 REPORT TYPE AND DATES COVERED
	October 1995	Final Report for Period October 1993 - October 1994

4 TITLE AND SUBTITLE
Demonstrations of a Pressure Sensitive Paint Data System in the AEDC Propulsion Wind Tunnel 16T

5 FUNDING NUMBERS
PE 62203F
JN 1872

6 AUTHOR(S)
Sellers, M.E., Micro Craft Technology/AEDC Operations

7 PERFORMING ORGANIZATION NAME(S) AND ADDRESS(ES)
Arnold Engineering Development Center/DOF
Air Force Materiel Command
Arnold Air Force Base, TN 37389-4000

8 PERFORMING ORGANIZATION REPORT NUMBER
AEDC-TR-95-8

9 SPONSORING/MONITORING AGENCY NAME(S) AND ADDRESS(ES)
Arnold Engineering Development Center/DOT
Air Force Materiel Command
Arnold Air Force Base, TN 37389-6000

10. SPONSORING/MONITORING AGENCY REPORT NUMBER

11. SUPPLEMENTARY NOTES
Available in Defense Technical Information Center (DTIC).

12A DISTRIBUTION/AVAILABILITY STATEMENT
Approved for public release; distribution is unlimited.

12B DISTRIBUTION CODE

13 ABSTRACT (Maximum 200 words)

A prototype Pressure Sensitive Paint (PSP) data system was assembled to demonstrate the capability to acquire and process surface pressure data using PSP in the AEDC Propulsion Wind Tunnel 16T. The first test was preformed on a 1/10-scale model of the Dornier Alpha Jet with a Transonic Technology (TST) Wing to obtain PSP data for comparison with conventional pressure measurements and Computational Fluid Dynamics (CFD) results. The second test was performed on a 15-percent scale model of the F-18 E/F to obtain PSP data on the upper and lower surface of the F-18 horizontal tail for comparison with conventional pressure measurements. Also, the PSP data were integrated to obtain loads on the horizontal tail for comparison with conventional pressure-integrated and balance-measured loads. A paint formulation developed at AEDC was used in the tests. Some of the unique features of the paint are discussed, and details of the data acquisition and reduction system are presented. The data system was controlled by the facility computer, which acquired PSP data automatically. The digitized images were processed to obtain qualitative images of the surface pressure distribution within minutes of acquisition. The images were processed further after the tests to obtain quantitative pressure data. Comparisons with measured pressure data, CFD solutions (TST only), and measured and integrated loads (F-18 only) are presented.

14 SUBJECT TERMS
Pressure Sensitive Paint, flow visualization, TST model, wind tunnel test, surface pressure distribution, F-18 E/F model, transonic flow, integrated forces and moments, spectral characteristics

15 NUMBER OF PAGES
66

16 PRICE CODE

17 SECURITY CLASSIFICATION OF REPORT	18 SECURITY CLASSIFICATION OF THIS PAGE	19 SECURITY CLASSIFICATION OF ABSTRACT	20 LIMITATION OF ABSTRACT
UNCLASSIFIED	UNCLASSIFIED	UNCLASSIFIED	SAME AS REPORT

CONTENTS

LLUSTRATIONS

TABLES

1.0 INTRODUCTION

Work is under way at the Arnold Engineering Development Center (AEDC) to develop a data acquisition system that will acquire surface pressure data on a wind tunnel model using Pressure Sensitive Paint (PSP). When illuminated by light at a specific wavelength, the PSP luminesces at another specific wavelength with an intensity that is inversely proportional to the local partial pressure of oxygen. Optical access to illuminate and visualize the model is a primary requirement for obtaining PSP data. The AEDC transonic wind tunnels have porous walls through which a part of the boundary layer is removed. As a result, the optical access is limited to small glass ports in the walls. A prototype data acquisition system was assembled that addressed the limited optical access while being interfaced with the facility computer to allow automatic PSP data acquisition.

During recent tests in the AEDC Propulsion Wind Tunnel 16T, the ability to acquire PSP data in a production environment was demonstrated using the prototype system. The first test was on a 1/10-scale model of the Dornier Alpha Jet with PSP applied to the upper surface of a Transonic Technology (TST) wing. Both PSP and conventional pressure data were acquired simultaneously at Mach numbers 0.6, 0.835, and 0.9 while angle of attack was varied from 0 to 8 deg. The second test was on a 15-percent scale model of the F-18 E/F with PSP applied to the upper and lower surface of one horizontal tail. PSP and conventional pressure data were acquired simultaneously at Mach numbers 0.6, 0.85, 0.95, and 1.2 while angle of attack was varied from 0 to 8 deg. The PSP images were processed using NASA-developed software, producing qualitative images of the surface pressure distribution within minutes of acquisition. After the test, the images were processed further to obtain quantitative pressure data.

1.1 BACKGROUND

The development of PSP in the U.S. has been performed most notably at NASA Ames Research Center in cooperation with the University of Washington, and at the McDonnell-Douglas Corporation. The paint developed at the University of Washington uses platinum octaethylporphyrin (PtOEP) suspended in Genessee® polymer binder GP-197. McDonnell-Douglas has developed a proprietary paint of unpublished composition. The paint developed at AEDC also uses PtOEP, but the PtOEP is not suspended in a binder. As described in Refs. 1 and 2, when the luminescent molecule (PtOEP or other) absorbs a photon of appropriate energy, the molecule enters an excited state. From this state, the molecule decays to the ground state through a series of transitions with at least one resulting in the emission of a photon. Fluorescence is the emission of a photon with a lifetime on the order of 10^{-8} sec and arises from a singlet transition. In contrast, phosphorescence is a delayed emission with a lifetime on the order of 10^{-3} to 100 sec and arises from a triplet-singlet transition. Most luminescent molecules emit very little fluorescence and strong phosphorescence (which is measured). A schematic of the lowest energy level transitions is shown

in Fig. 1. Since the energy decay resulting in the photon emission is never complete, the emitted photon will have less energy, and, therefore, a longer wavelength than the original exciting photon. The shift in emission wavelength from the absorption wavelength permits the measurement of emission intensity, or luminescence, with the use of appropriate filters. An alternate transition to the ground state is provided by collision with an oxygen molecule. Rather than emitting a photon, the excess energy of the luminescent molecule is absorbed by the oxygen molecule during a collisional deactivation. Increasing amounts of oxygen increase the collisional deactivations, resulting in a decrease in the amount of luminescence. Since the number of oxygen molecules is directly proportional to the local pressure, low-pressure regions on the surface of a model will be brighter than those of high pressure. The process can be modeled using a simplified form of the Stern-Volmer relation:

$$\frac{I_0}{I} = 1 + K_q P_{O_2} \tag{1}$$

where I_0 is the PSP luminescence in the absence of oxygen, I and P_{O_2} are the PSP luminescence and partial pressure of oxygen at some pressure, and K_q is the Stern-Volmer constant. Presented in Fig. 2 is a graphic representation of the inverse of Eq. (1) for several Stern-Volmer constants. Paints with a large K_q have higher sensitivity at low absolute pressures and lower sensitivity at high absolute pressures. Paints with a small K_q have a lower, but more constant, sensitivity across the pressure range. The AEDC PSP has a large K_q (approximately 0.9 at room temperature), which performs well at pressures near and below 0.5 atm, but does not have enough sensitivity to measure pressures accurately near or above 1 atm.

Equation (1) does not include the terms for temperature sensitivity since it is not possible, at this time, to obtain the temperature distribution simultaneously with the pressure distribution. The PtOEP paint formulations have varying sensitivities to changes in temperature. The temperature sensitivities of the AEDC PSP and PtOEP in GP-197 are presented in Fig. 3. The reference luminescence and pressure values for each paint were acquired at 1 atm and 25°C.

The major advantages of using PSP are to provide a complete surface pressure distribution and to obtain information in areas where it is not possible to install pressure orifices. However, a limited number of orifices may be needed on the model to calibrate or verify the PSP data, as well as in areas that cannot be seen by the cameras.

2.0 APPARATUS

2.1 TEST ARTICLES

Details of the TST model are presented in Fig. 4. The starboard wing was instrumented with chordwise rows of pressure taps at 5 span stations. The top surface of the port wing was painted with the AEDC PSP. The wing pressure orifice designation and location are listed in Table 1.

A sketch showing the F-18 E/F horizontal tail pressure orifice distribution is presented in Fig. 5. The starboard horizontal tail was instrumented with chordwise rows of pressure taps at 8 span stations. The horizontal tail pressure orifice designation and location are listed in Table 2. The port horizontal tail was gaged with a 5-component balance to measure the tail loads, and painted with the AEDC PSP.

2.2 PRESSURE SENSITIVE PAINT

Two layers of paint typically are applied to the model surface. The first is a white substrate that helps reflect the luminescent light away from the model surface. Most paint formulations use some type of epoxy paint, but the AEDC formulation uses Very High Temperature (VHT) paint as the substrate. The second, the PSP layer, contains the luminescent molecule and is applied over the substrate. When suspended in GP-197, the PtOEP molecule becomes oxygen sensitive. The PtOEP in GP-197 does not interact with the substrate and can be applied over any type of white epoxy paint. However, with the AEDC PSP, the PtOEP is not suspended in a binder and is not oxygen sensitive until sprayed onto the VHT. The AEDC PSP bonds with the VHT and is exposed directly to oxygen molecules. As a result, there is no luminescence delay (induction period) when the paint is illuminated, and the response to pressure change is almost instantaneous. The induction period for PtOEP in GP-197 has been documented by Uibel (Ref. 3) and can require up to 10 min to reach luminescent equilibrium after exposure to the excitation light. Also, the oxygen molecules must permeate through the GP-197, resulting in a luminescent lag as surface pressure changes.

Photodegradation is a decrease in luminescence over time while exposed to light and is a major source of error with some paints. The photodegradation rates for the AEDC PSP and PtOEP in GP-197 are presented in Fig. 6. The absence of a binder in the AEDC PSP decreases the photo-degradation rate significantly and eliminates the induction effect. Most of the currently available paints require more than 24 hours to apply the substrate and PSP while the AEDC substrate and PSP can be applied in approximately 5 hours.

7

2.3 PSP DATA SYSTEM

A schematic of the PSP data acquisition and processing system used during the TST test is shown in Fig. 7. The upper surface of the port wing was painted with the AEDC PSP and illuminated with xenon-arc lamps. A cold mirror set at 45-deg incidence to the light reflected 90 percent or more of light between 325 and 475 nm through a short wave pass (SWP) dichroic filter designed to pass wavelengths below 500 nm. The filtered light from the xenon-arc lamps passed through optics which spread the light to a diameter of approximately 2 ft at the tunnel centerline. A shutter placed in front of each lamp was opened to pass light while images were being acquired. The luminescent light emitted by the paint passed to the camera through a hot mirror designed to reflect light above 700 nm, and a long wave pass (LWP) dichroic filter designed to pass light above 550 nm. A conventional video camera was used to obtain black-and-white images of the luminescent surface. The camera automatic gain control and black level were disabled. The camera output was digitized at 512 × 480 pixel spatial resolution and 8-bit grey level resolution using a frame-grabber board mounted inside a personal computer (PC). The camera output was also sent to a laser disc video recorder capable of continuous recording at 30 frames/sec.

The PtOEP absorption and emission spectral characteristics are presented in Fig. 8, along with the filtered light source spectrum. Each spectrum was normalized by its peak output. Note that the cold mirror and SWP filter prematurely cut off excitation light that would have provided more luminescence. Also, some of the excitation light in the 620- to 700-nm range (in the PtOEP emission band) passed through the cold mirror and SWP filter, resulting in a reduction of the camera signal-to-noise ratio (SNR) because of reflected excitation light.

The PSP data system used for the F-18 E/F test was an improved and expanded version of that described above. The cold mirror was rotated to 67.5-deg incidence to the incoming light and the 500-nm SWP filter was changed to a 550-nm SWP filter. Also, the 550-nm LWP filter on the camera was changed to a 600-nm LWP filter. The results presented in Fig. 9 show a significant increase in the excitation bandwidth and elimination of the light source in the emission band. Two new video cameras were used to acquire images of the upper and lower surface of the horizontal tail. The camera outputs were digitized at 628 × 474 pixel spatial resolution and 8-bit grey level resolution using a new frame grabber board. The laser disc video recorder was not used.

3.0 PROCEDURES

3.1 TEST CONDITIONS

The TST test was conducted at nominal Mach numbers of 0.6, 0.835, and 0.9 at a Reynolds number of 2.3 million per ft. The F-18 E/F test was conducted at nominal Mach numbers of 0.6,

0.85, 0.95, and 1.2 at a Reynolds number of 3.0 million per ft. The angle of attack was varied from 0 to 8 deg during both tests.

3.2 DATA ACQUISITION

Two methods of data acquisition were used during the TST test. In the first, acquisition of conventional pressure data and PSP images was performed automatically under the control of the facility computer. The facility computer set the requested model attitude and signaled the PC to acquire the PSP images while the facility computer acquired the conventional pressure data. The PC commanded the power supplies for the xenon-arc lamps to increase to full power and the shutter in front of each lamp to open. Four images, 1/30-sec apart, were acquired and stored on the PC hard drive. After the images were acquired, the shutters were closed and the lamps were reduced to half power. The PC returned a signal, indicating the images had been stored, which allowed the facility computer to move the model to the next attitude. The images stored on the PC hard drive were transferred to the workstation via floppy disk. The second data acquisition method pitched the model at a constant rate while recording images from the camera at 30 frames/sec onto the laser disc video recorder. The model was pitched at a constant rate of approximately 0.75 deg/sec, resulting in images approximately every 0.025 deg. The shutters remained open and power supplies at full power while the model was pitched. The conventional pressure data could not be acquired while the model was pitched continuously. The images were stored on the laser disc primarily for flow visualization purposes.

With the exception of continuous pitch image acquisition, the data acquisition process described above was also used during the F-18 E/F test. However, since two cameras were used, the image acquisition process was staged to first obtain data on the top surface and then on the lower surface. The lamp power and shutters were staged with the image acquisition sequence. A new frame grabber board was used to acquire 16 images, 1/30-sec apart, that were averaged in memory on the board for each camera. The averaged images were stored on the workstation hard drive via ethernet. Also, a file containing the conventional pressure data was transferred from the facility computer to the workstation via ethernet.

3.3 PSP DATA REDUCTION

Determining I_0 in Eq. (1) is not practical in the wind tunnel environment. As described in Ref. 1, ratioing the intensities of an image at a known reference (wind-off) condition to an operating (wind-on) condition eliminates the need to determine I_0. Also, the effects of nonuniformities in illumination and paint thickness on the amount of luminescence are eliminated. The ratio of wind-off to wind-on intensities using Eq. (1) is:

$$\frac{I_0/I}{I_0/I_{ref}} = \frac{I_{ref}}{I} = \frac{1 + K_q P}{1 + K_q P_{ref}} \tag{2}$$

where I_{ref} and P_{ref} are the PSP luminescence and pressure at a known wind-off condition, and I and P are the PSP luminescence and surface pressure at the wind-on condition. The surface pressure can then be determined from:

$$P = A + B\frac{I_{ref}}{I} \tag{3}$$

where A and B are the calibration coefficients for the paint. Taking the ratio of wind-off to wind-on intensities assumes the model position and shape in the image remain constant. However, at the wind-on condition, the model moved in the field of the camera as a result of deflections from operating loads. Using the image registration technique described by Bell (Ref. 4), small targets were placed on the surface at known coordinates so that the wind-on image could be stretched and shifted (registered) to match the wind-off image. The ratio of the wind-off intensities to the registered wind-on intensities (I_{ref} / I) was computed for each pixel in the image. The constants A and B were determined from a least-squares fit of the conventional pressure data and intensity ratio data at known corresponding locations on the model surface. These constants were used to convert intensity ratio to surface pressure coefficient (CP) over the painted surface and are presented in Table 3. The registration marks were also used to relate the 2-D image coordinate system to the 3-D model coordinate system. After the test, the photogrammetry methods described by Bell (Ref. 4) were used to overlay the 2-D images onto a 3-D mesh grid of the model surface. A file was generated with pressure coefficient data at each mesh point to permit display of the pressure coefficient distribution using color contours. In addition, the F-18 E/F PSP data were integrated to determine horizontal tail normal force and pitching and hinge moments using typical CFD integration methods.

4.0 RESULTS AND DISCUSSION

4.1 TST TEST

A comparison of pressure coefficient (CP) data from conventional pressure and PSP measurements versus wing chord position (X/C) is presented in Fig. 10. The PSP data agreed well with the conventional pressure data at Mach numbers 0.835 and 0.9, where the surface pressure was low. The data SNR decreased as pressure increased, primarily because of the decrease in luminescence and increasing influence of reflected excitation light in the emission band. The excitation light leakage in the emission band is considered to be the main source of error in the PSP pressure data. As a consequence of these effects, the Mach number 0.6 data at the corresponding higher pressures did not agree as well as the higher Mach number data (lower pressures). The image used for I_{ref} in Eq. (3) was obtained at 400 psfa to increase the SNR.

Comparisons of PSP data and thin-layer Navier-Stokes solutions, using a Baldwin-Lomax (Ref. 5) turbulent model over the entire wing, are presented in Fig. 11. The flow-field solution was generated using the Chimera overset grid approach (Ref. 6). The agreement is very good with the exception of data at the wing root and tip. Also, at 6-deg angle of attack, the flow-field physics downstream of the wing notch were not modeled adequately. The CFD solution difference at the wing root is the result of using Euler equations over the fuselage rather than Navier-Stokes equations.

4.2 F-18 E/F TEST

A comparison of CP data from conventional pressure and PSP measurements versus wing chord position (X/C) for the upper and lower F-18 E/F horizontal tail surfaces is presented in Fig. 12. The pressure data at Mach number 0.6 does not compare well, primarily because of the associated higher pressure level. The test was run at a higher total pressure than was desired because the horizontal tail balance failed prior to testing the PSP. Consequently, the tunnel conditions which had been set in previous testing were repeated during the PSP test to permit comparison of the PSP and conventional pressure integrated loads with the balance measurements. The agreement of the PSP data with the conventional pressure data is good at Mach numbers 0.85, 0.95, and 1.2, except at the tip of the horizontal tail (rows 7 and 8). As described above, the camera SNR decreased as pressure increased and is considered to be the main source of error. A sample of data used to determine the constants A and B in Eq. (3), and the resulting curve fit, are presented in Fig. 13. In this example, lower surface data for rows 7 and 8 (at the tip) do not fall in line with the general data trend. As a result, these rows were not included in the least-squares calculation and will therefore not agree well with the conventional pressure data. Also, separate curve fit coefficients were determined for the upper and lower surfaces when two distinctly different trends existed. The scatter in Fig. 13 is indicative of the signal noise and the data uncertainty.

Integrated loads comparisons are presented in Fig. 14. The PSP-integrated loads agreed well with conventional pressure-integrated and balance-measured loads at Mach numbers 0.85, 0.95, and 1.2. PSP-integrated loads at Mach number 0.6 have considerable scatter because the PSP pressure resolution was insufficient.

Color contours showing the global variation in surface pressure for PSP and conventional pressure measurements are presented in Fig. 15. The data from the conventional pressure measurements were not extrapolated to the surface edges (indicated by the white line). PSP pressure data were determined at 3,431 evenly distributed points on each surface of the horizontal tail, as compared with 124 points on each surface of the instrumented horizontal tail.

5.0 SUMMARY

A prototype Pressure Sensitive Paint (PSP) data system was demonstrated in the AEDC Propulsion Wind Tunnel 16T on tests involving a Dornier Alpha Jet model with a Transonic Technology (TST) wing and the F-18 E/F Jet Effects model. PSP data were acquired automatically under the control of the facility computer and processed to obtain qualitative images within minutes of acquisition. Some conclusions and observations from the demonstration tests are as follows:

- The AEDC PSP response to change in pressure is almost instantaneous and has no induction delay.

- Improvements made after the TST test to the paint illumination system increased the signal-to-noise ratio by increasing the excitation bandwidth and eliminating the passage of excitation light in the emission band.

- The PSP and conventional pressure data agreed well at higher Mach numbers where the surface pressures were low.

- The combination of low signal-to-noise ratio for the paint and 8-bit camera resolution resulted in poor measurement of pressure data at the higher pressures associated with Mach number 0.6.

- The F-18 E/F PSP integrated loads agreed well with conventional pressure-integrated and balance-measured loads at the higher Mach numbers.

New camera technology and paint formulations show high promise to increase pressure measurement accuracy when PSP is used. Future development programs will benefit from PSP technology by permitting the acquisition of pressure loads data on models without extensive pressure instrumentation, resulting in a compressed development schedule and significant cost reduction.

REFERENCES

1. McLachlan, B.G., et al. "Pressure Sensitive Paint Use in the Supersonic High-Sweep Oblique Wing (SHOW) Test." AIAA Paper 92-2686, AIAA 10th Applied Aerodynamics Conference, Palo Alto, California, June 1992.

2. Morris, M. J., et al. "Aerodynamic Applications of Pressure-Sensitive Paint." AIAA Paper 92-0264, 30th AIAA Aerospace Sciences Meeting, Reno, Nevada, January 1992.

3. Uibel, R., et al. "Video Luminescent Barometry: The Induction Period." AIAA Paper 93-0179, 31st Aerospace Sciences Meeting, Reno, Nevada, January 1993.

4. Bell, J. H. and McLachlan, B. G. "Image Registration for Luminescent Paint Sensors." AIAA Paper 93-0178, 31st Aerospace Sciences Meeting, Reno, Nevada, January 1993.

5. Baldwin, B. S. and Lomax, H. "Thin Layer Approximation and Algebraic Model for Separated Turbulent Flows." AIAA Paper 78-257, 16th Aerospace Sciences Meeting, Huntsville, Alabama, January 1978.

6. Benek, J. A., Steger, J. L., Dougherty, F. C., and Buning, P. G. "Chimera: A Grid-Embedding Technique." AEDC-TR-85-64 (AD-A167466), April 1986.
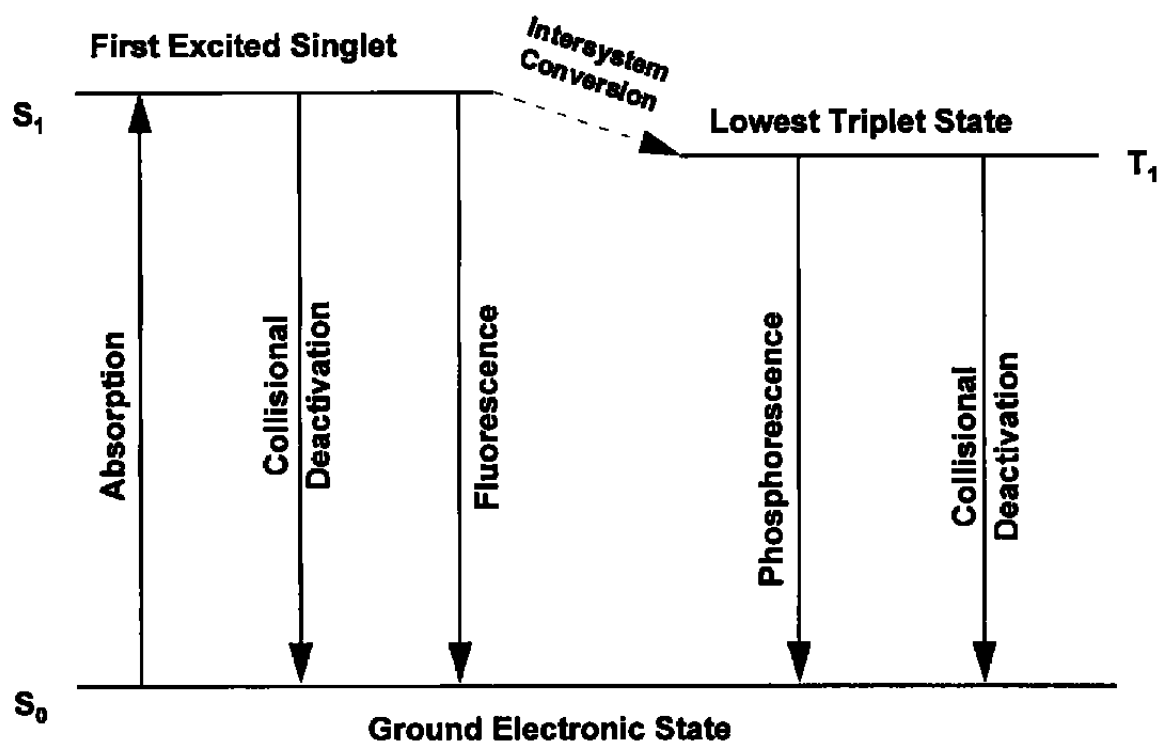
Figure 1. Basic luminescence process.
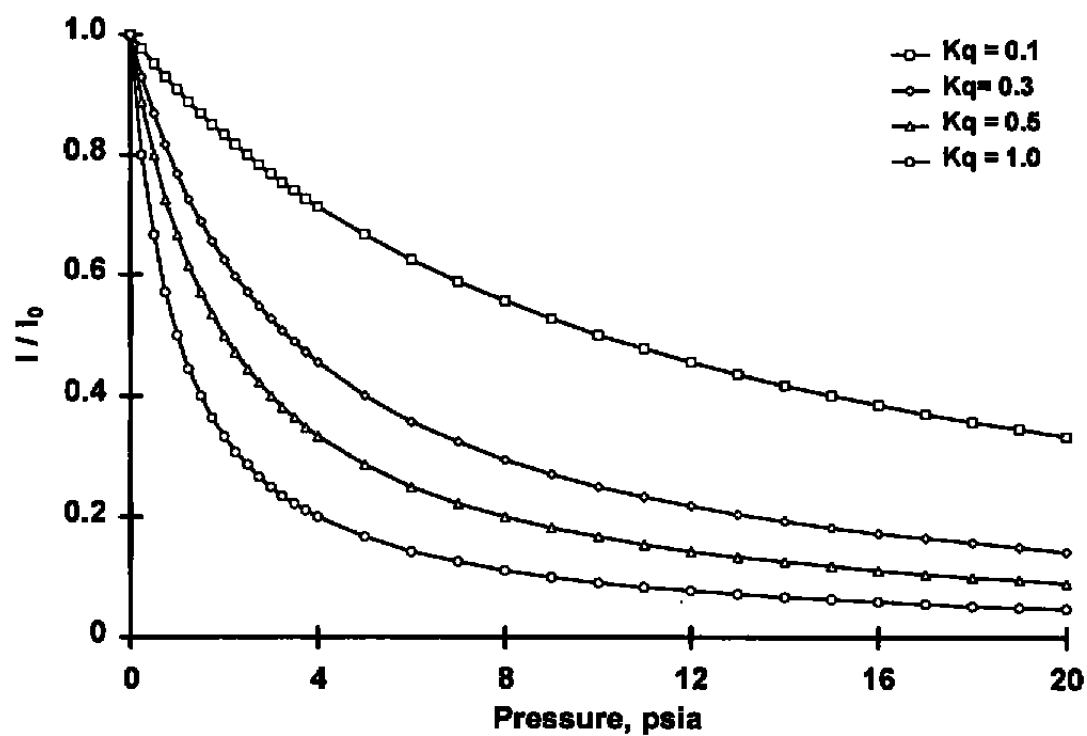
Figure 2. Luminescence as described by the Stern-Volmer Model.
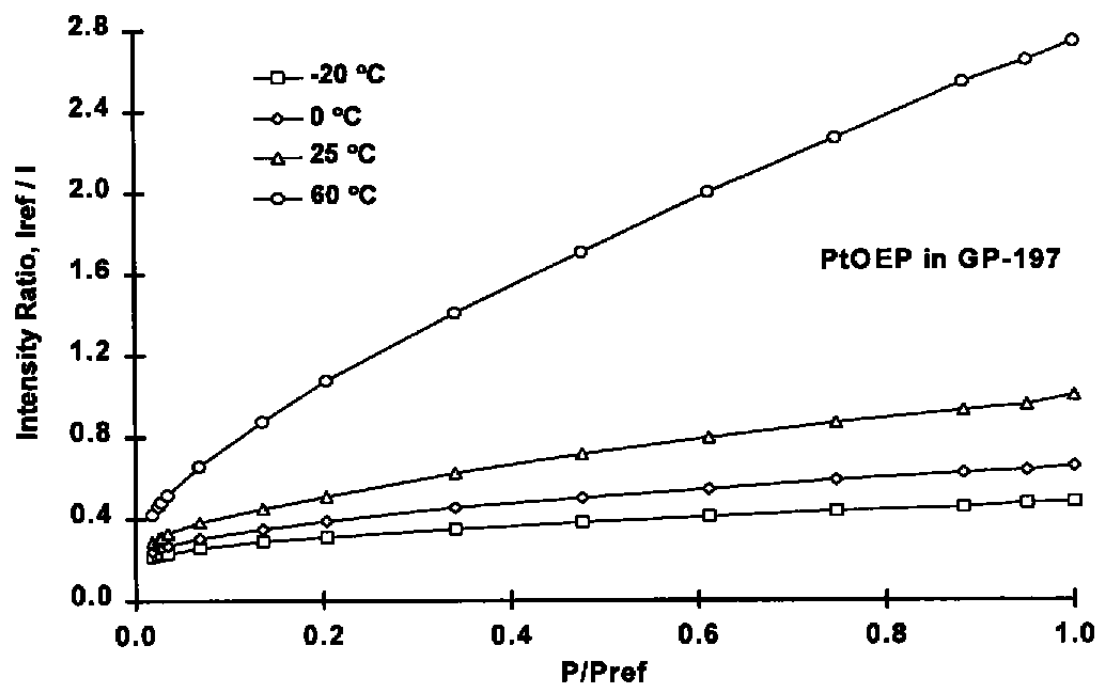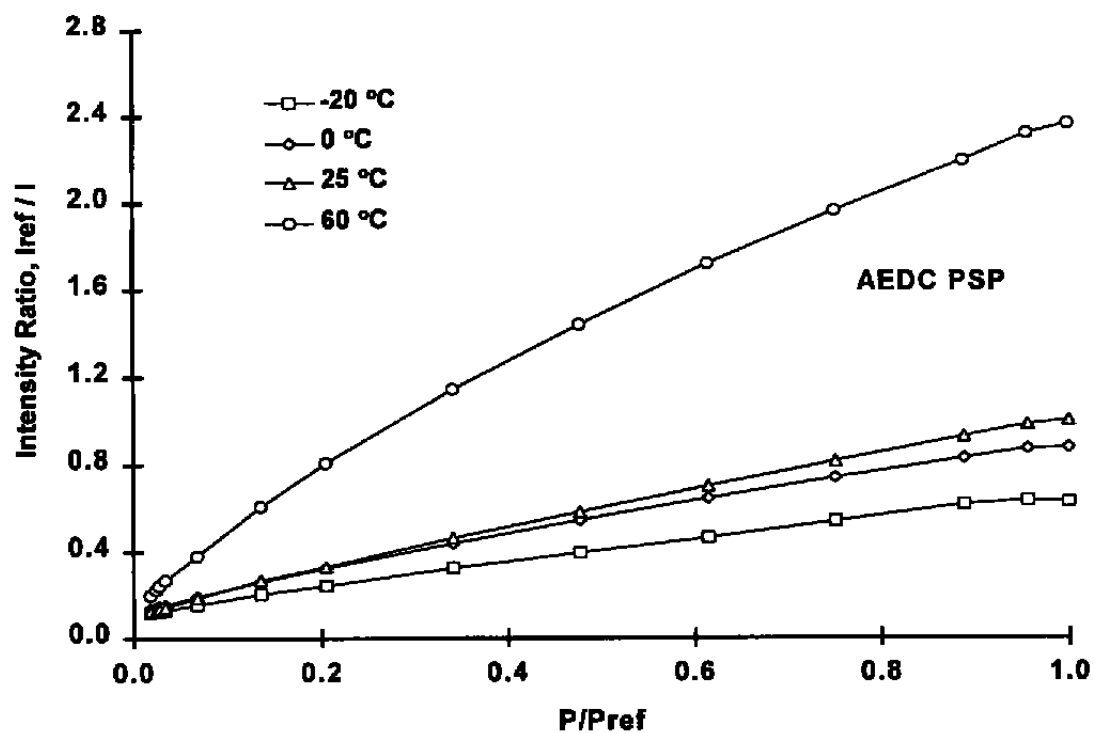
Figure 3. PSP temperature sensitivity.

Anhedral = -6 deg

Anhedral = -9 deg

46.643

35.881

9.843

46.102

17.032

Dimensions in Inches
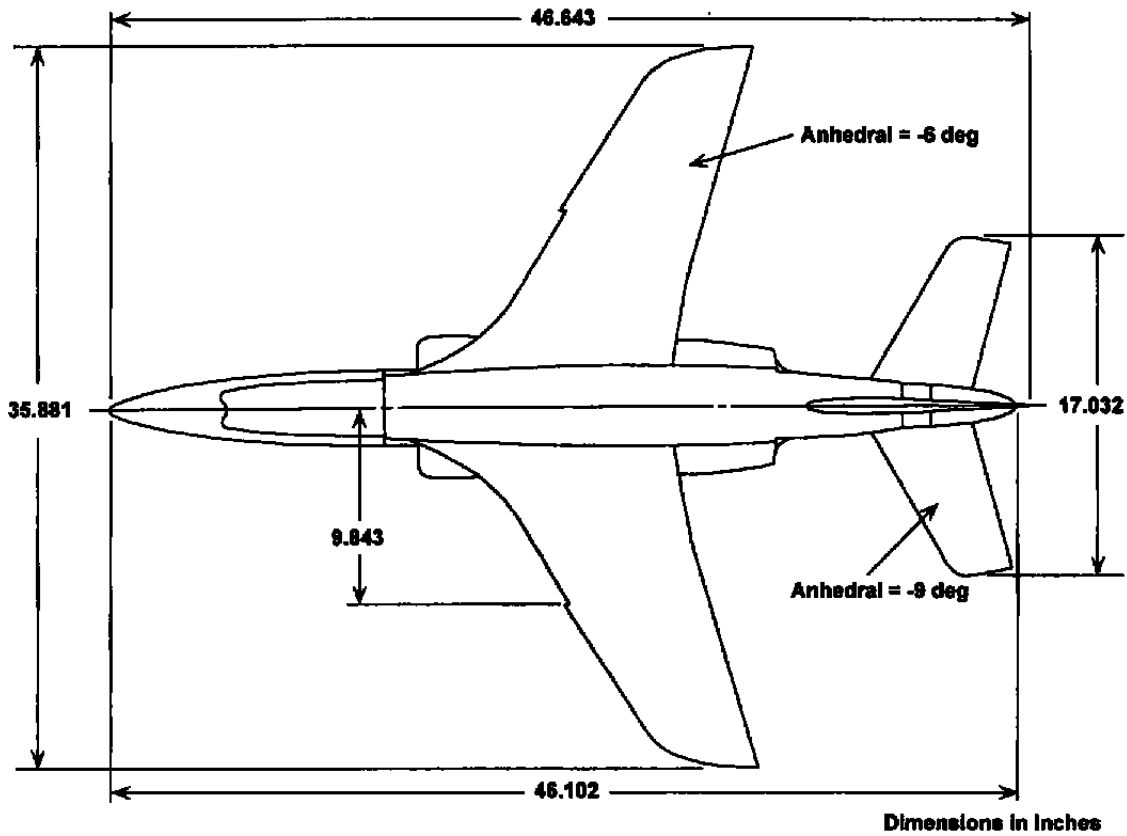
a. Test article dimensions

Figure 4. TST model.
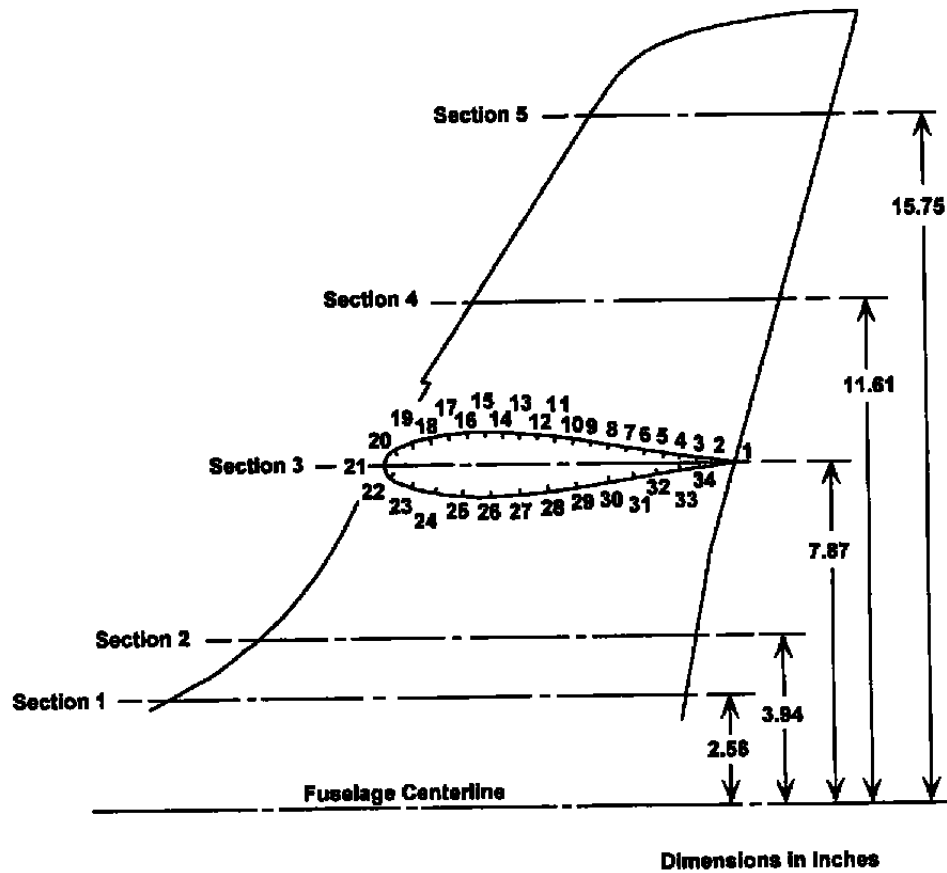
b. Wing pressure orifice distribution
Figure 4. Concluded.

19
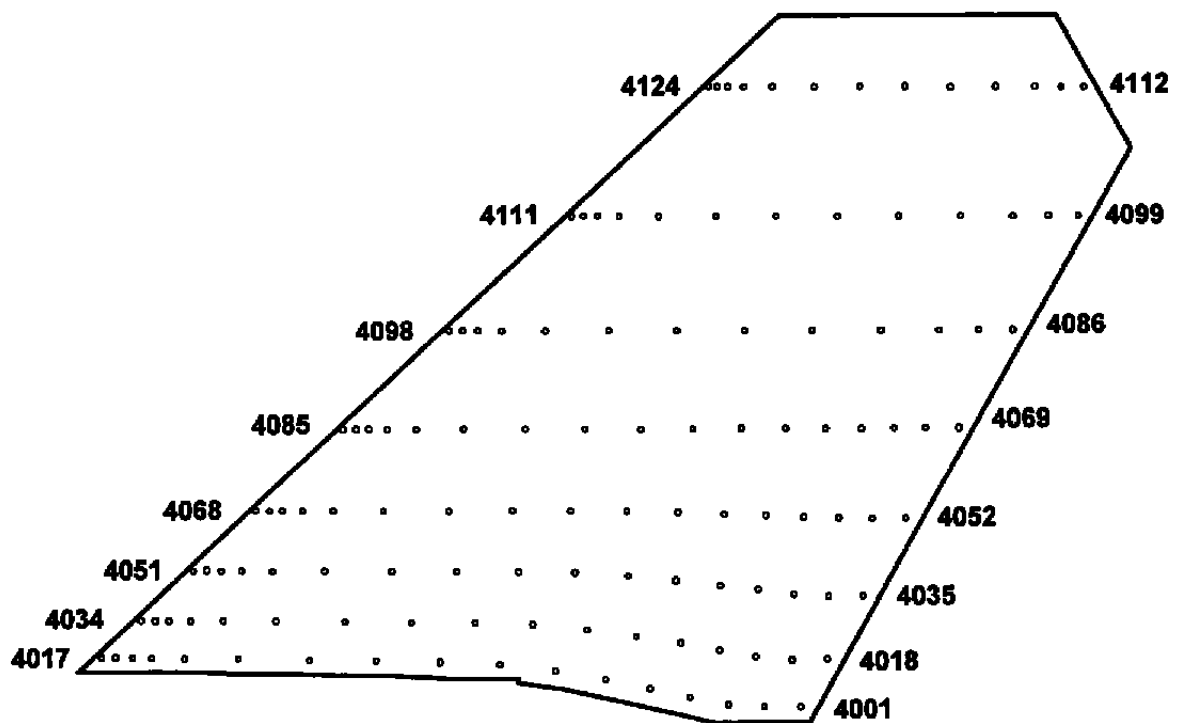
a. Upper surface pressure orifice locations
Figure 5. F-18 E/F horizontal tail.
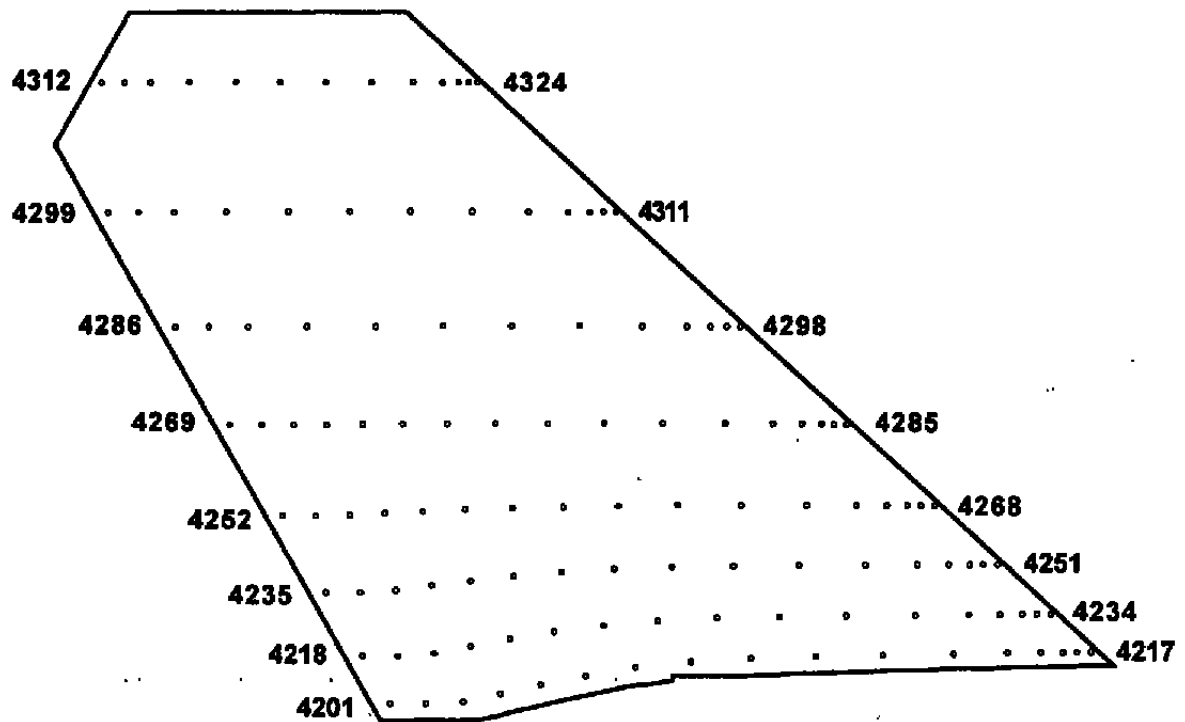
b. Lower surface pressure orifice locations

Figure 5. Concluded.
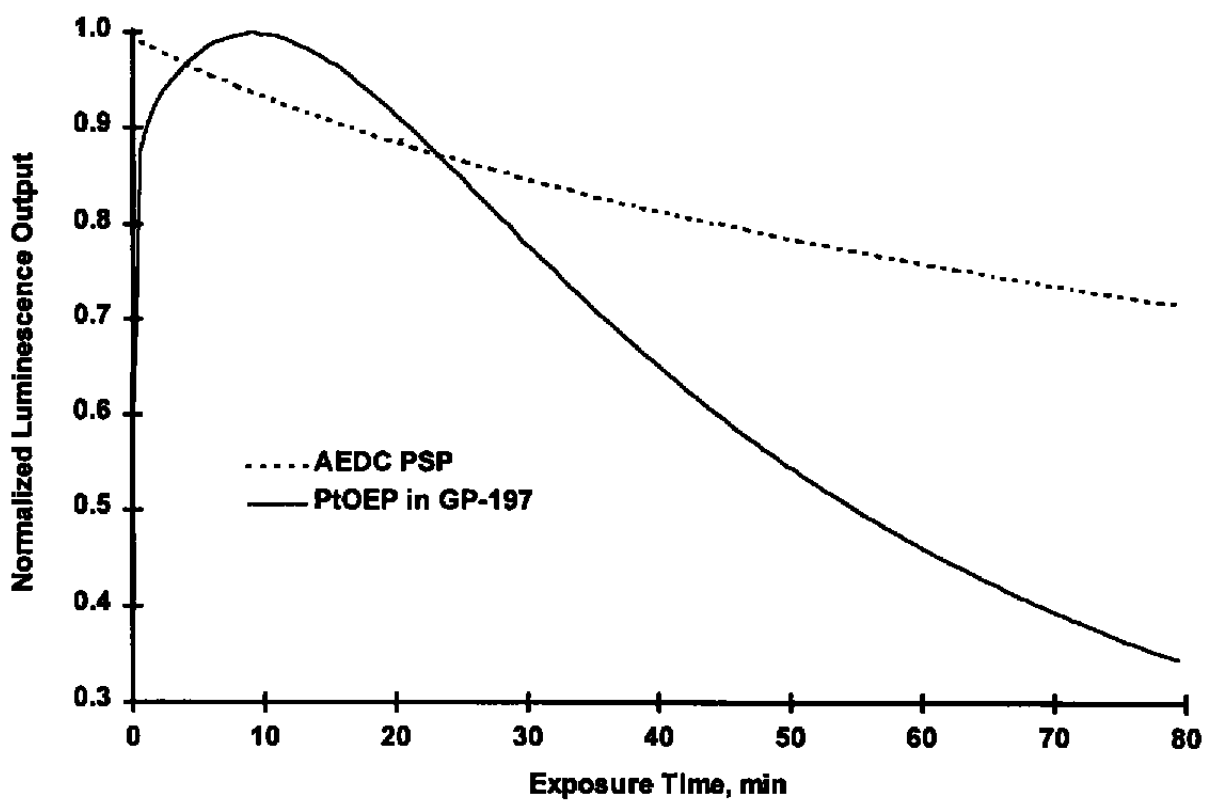
Figure 6. PtOEP photodegradation.

Figure 7. PSP data system.

Light Source ····· PtOEP Absorption — ··· PtOEP Emission
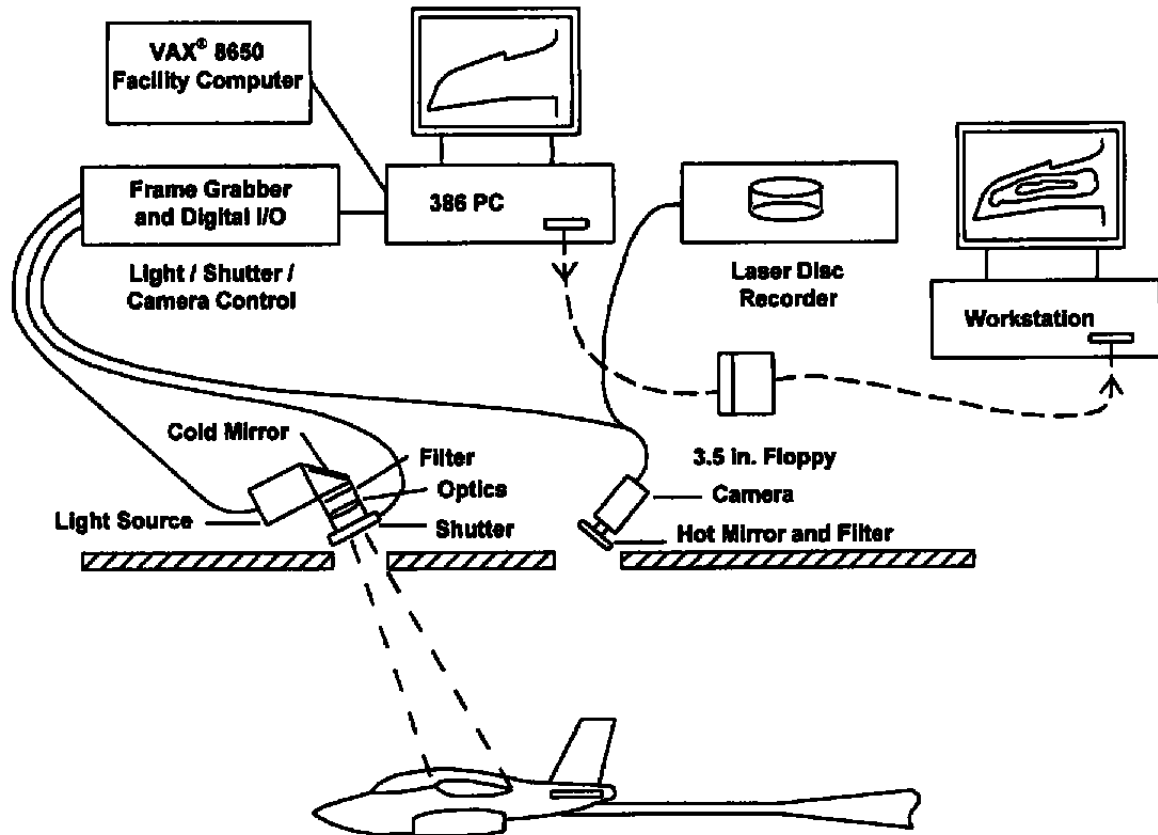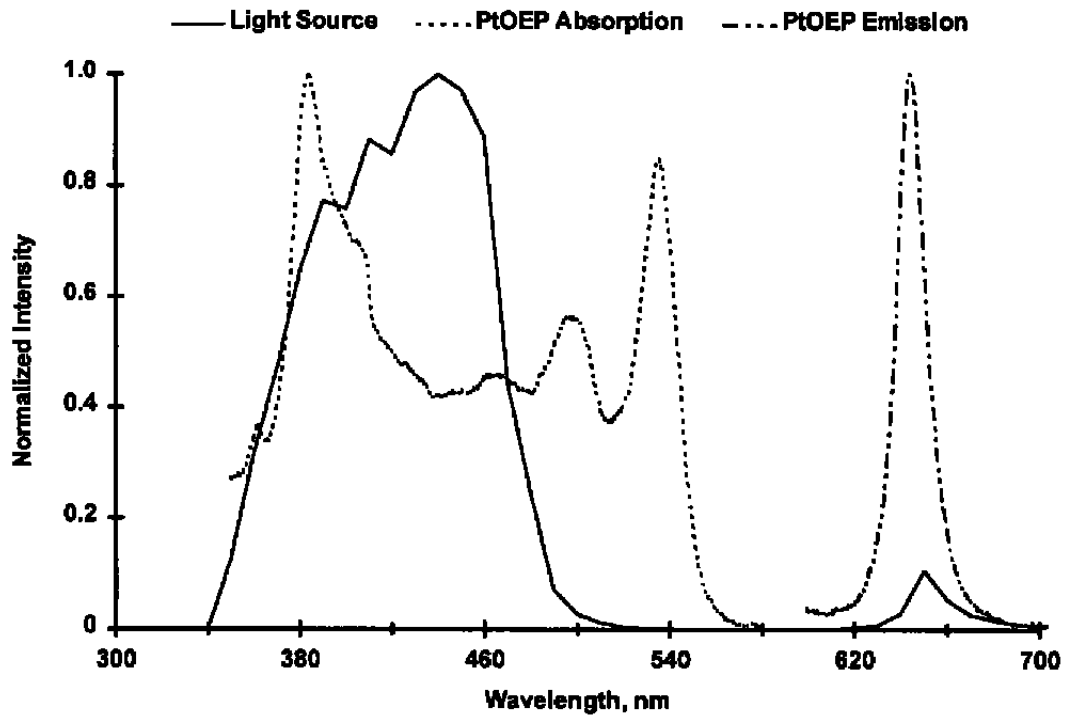
Figure 8. Spectral characteristics during TST test.

Light Source ····· PtOEP Absorption — ··· PtOEP Emission
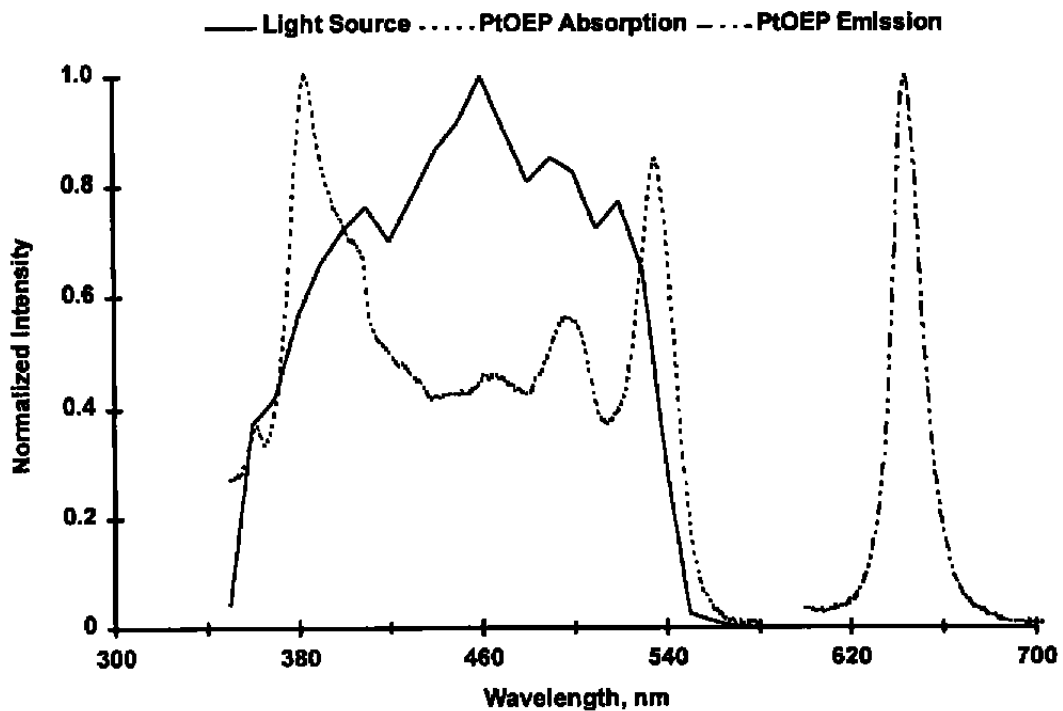
Figure 9. Spectral characteristics during F-18 E/F test.
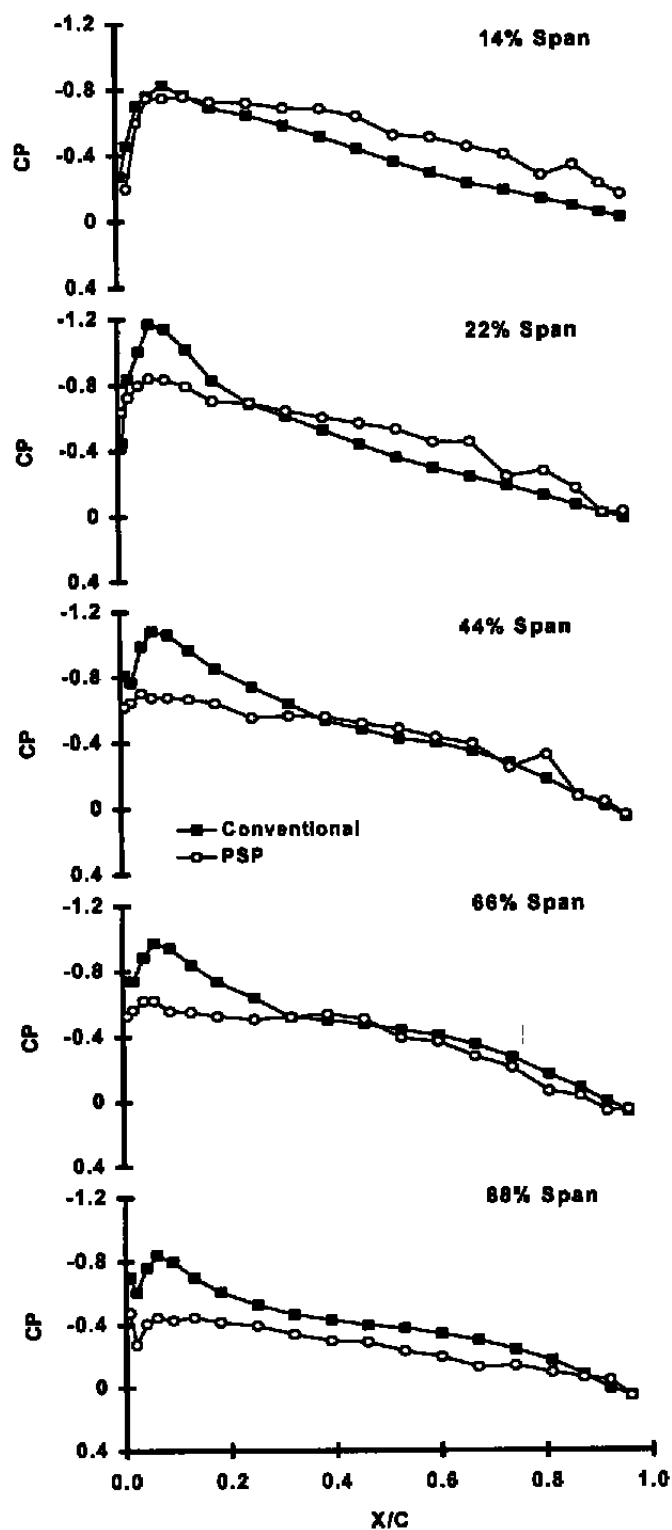
a. Mach = 0.6, Alpha = 4 deg

Figure 10. TST conventional and PSP pressure coefficient comparison.
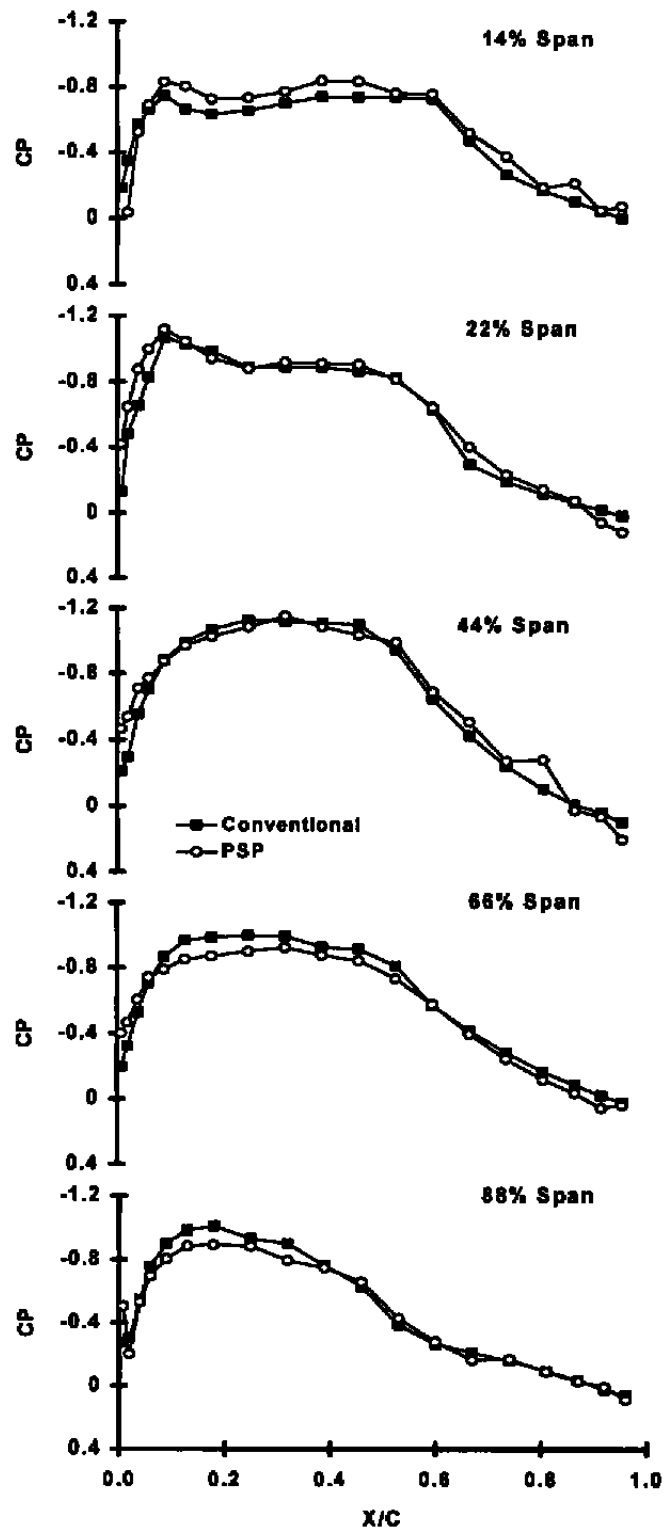
b. Mach = 0.835, Alpha = 4 deg
Figure 10. Continued.
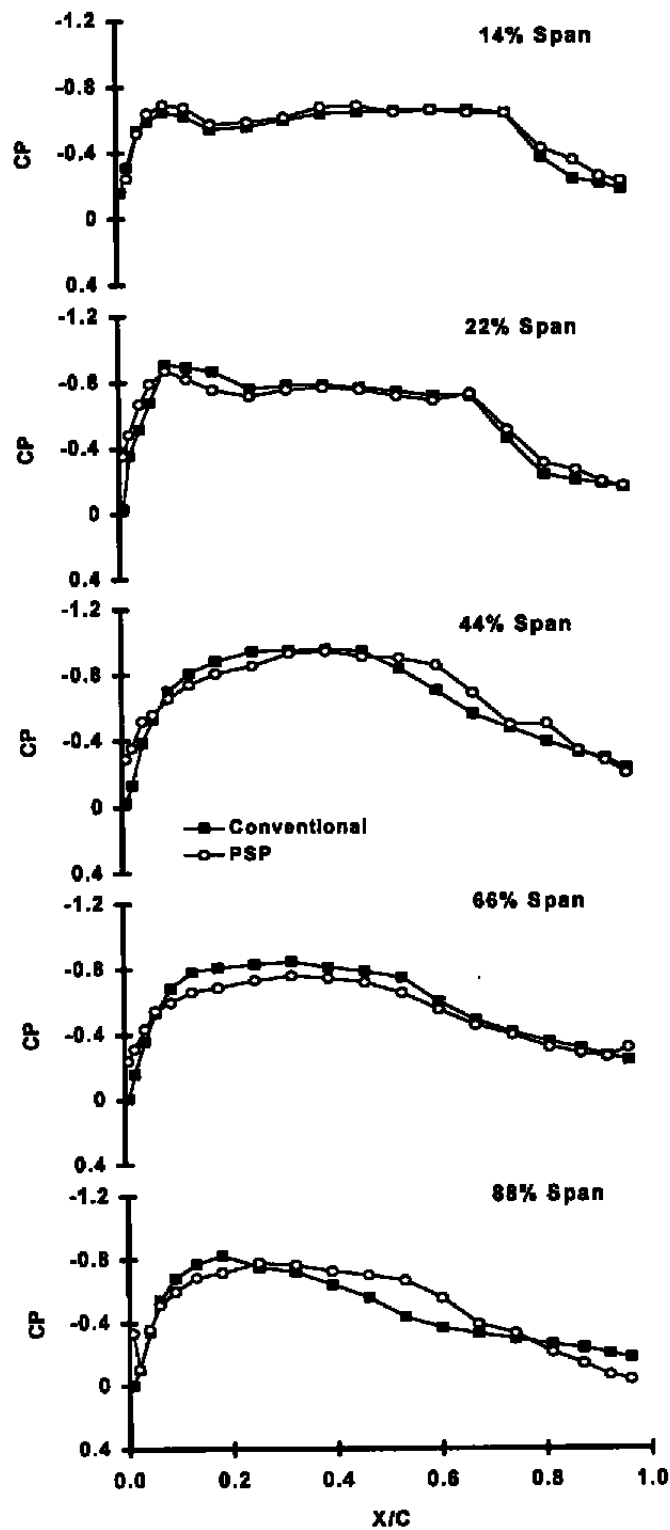
c. Mach = 0.9, Alpha = 4 deg
Figure 10. Concluded.
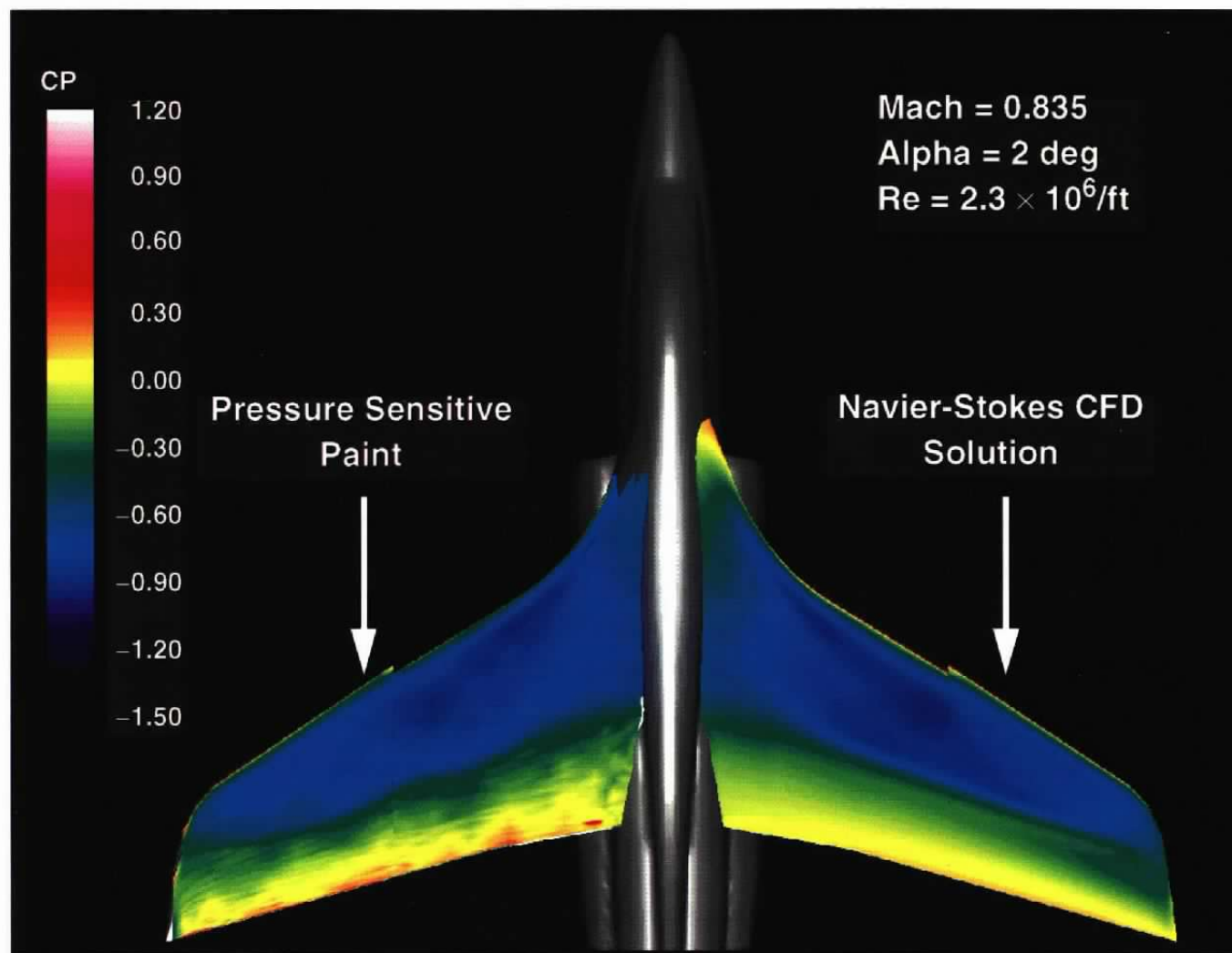
a. Mach = 0.835, Alpha = 2 deg

Figure 11. TST PSP and CFD pressure coefficient comparison.

CP

1.20
0.90
0.60
0.30
0.00
-0.30
-0.60
-0.90
-1.20
-1.50

Mach = 0.835
Alpha = 4 deg
Re = 2.3×10^6/ft

Pressure Sensitive
Paint

Navier-Stokes CFD
Solution
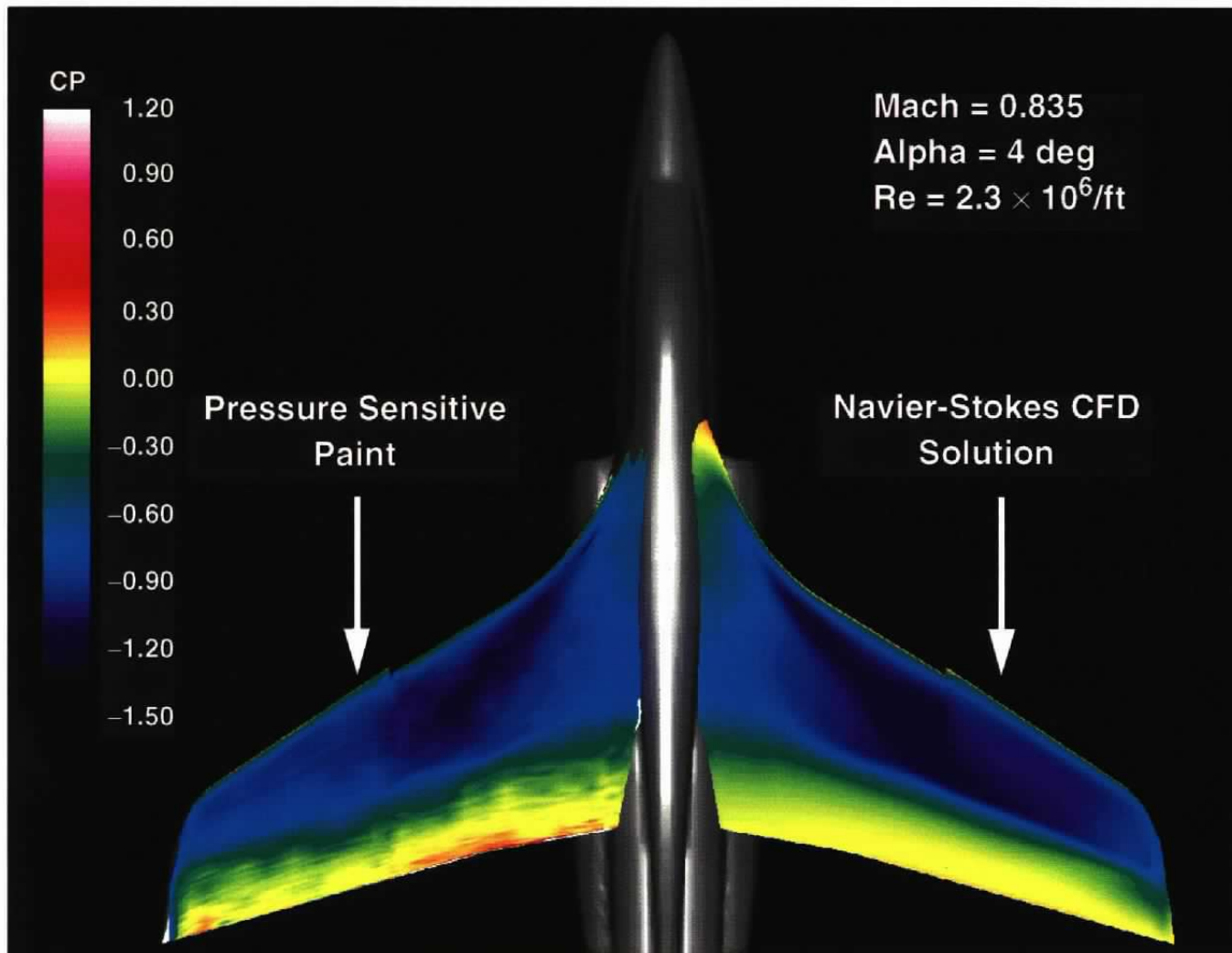
b. Mach = 0.835, Alpha = 4 deg
Figure 11. Continued.
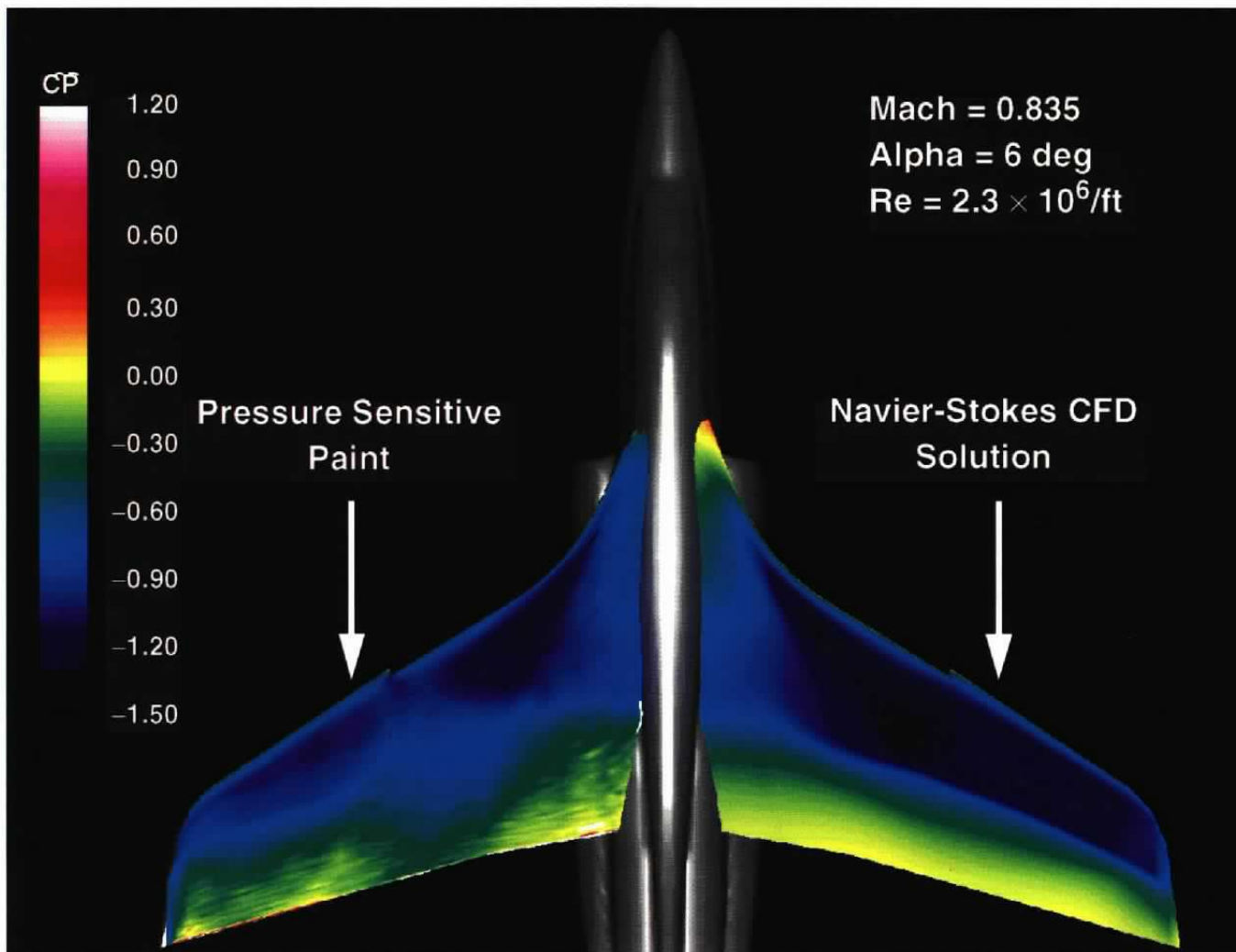
c. Mach = 0.835, Alpha = 6 deg
Figure 11. Concluded.
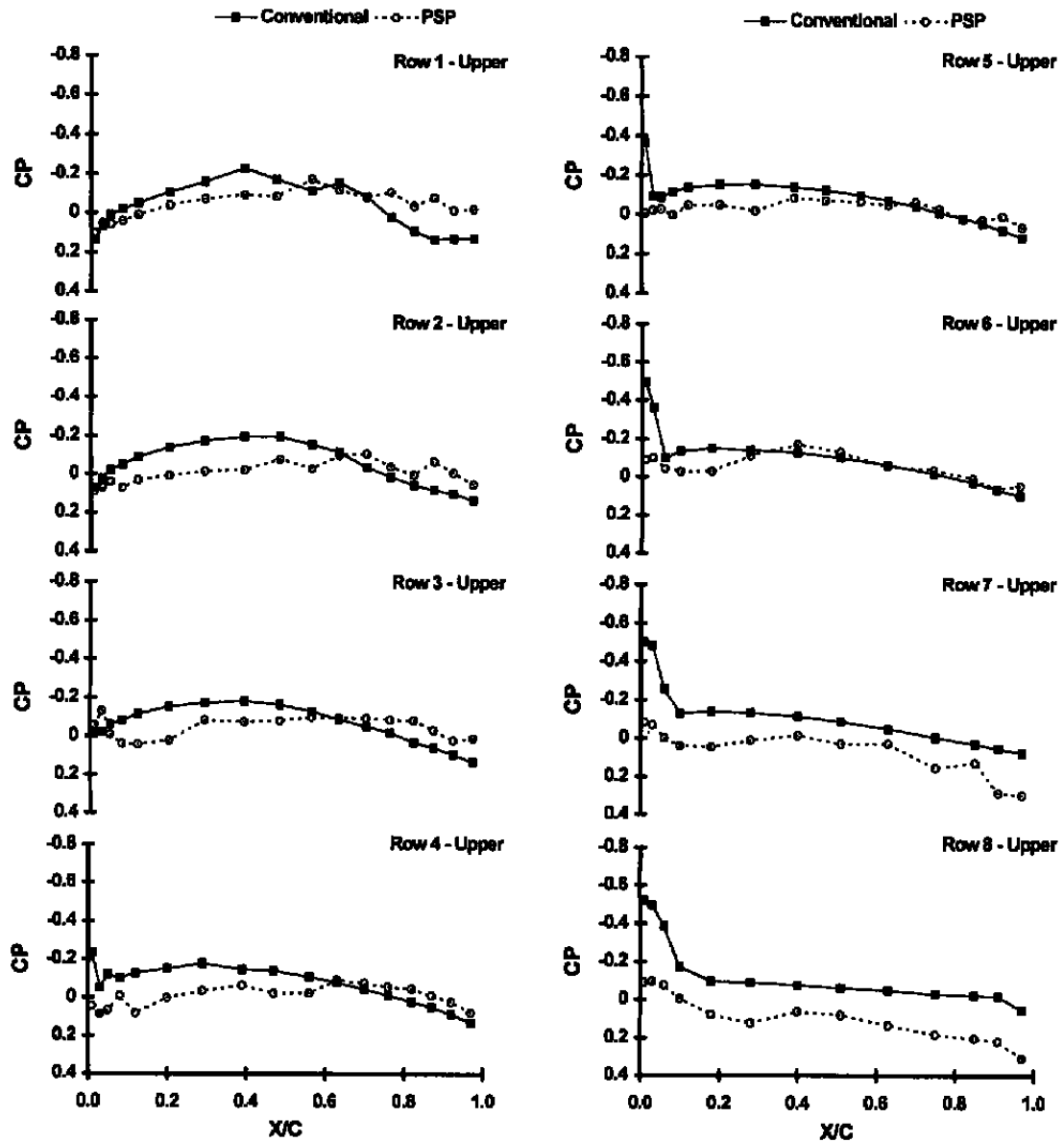
a. Horizontal tail upper surface, Mach = 0.6, Alpha = 6 deg

Figure 12. F-18 E/F conventional and PSP pressure coefficient comparison.
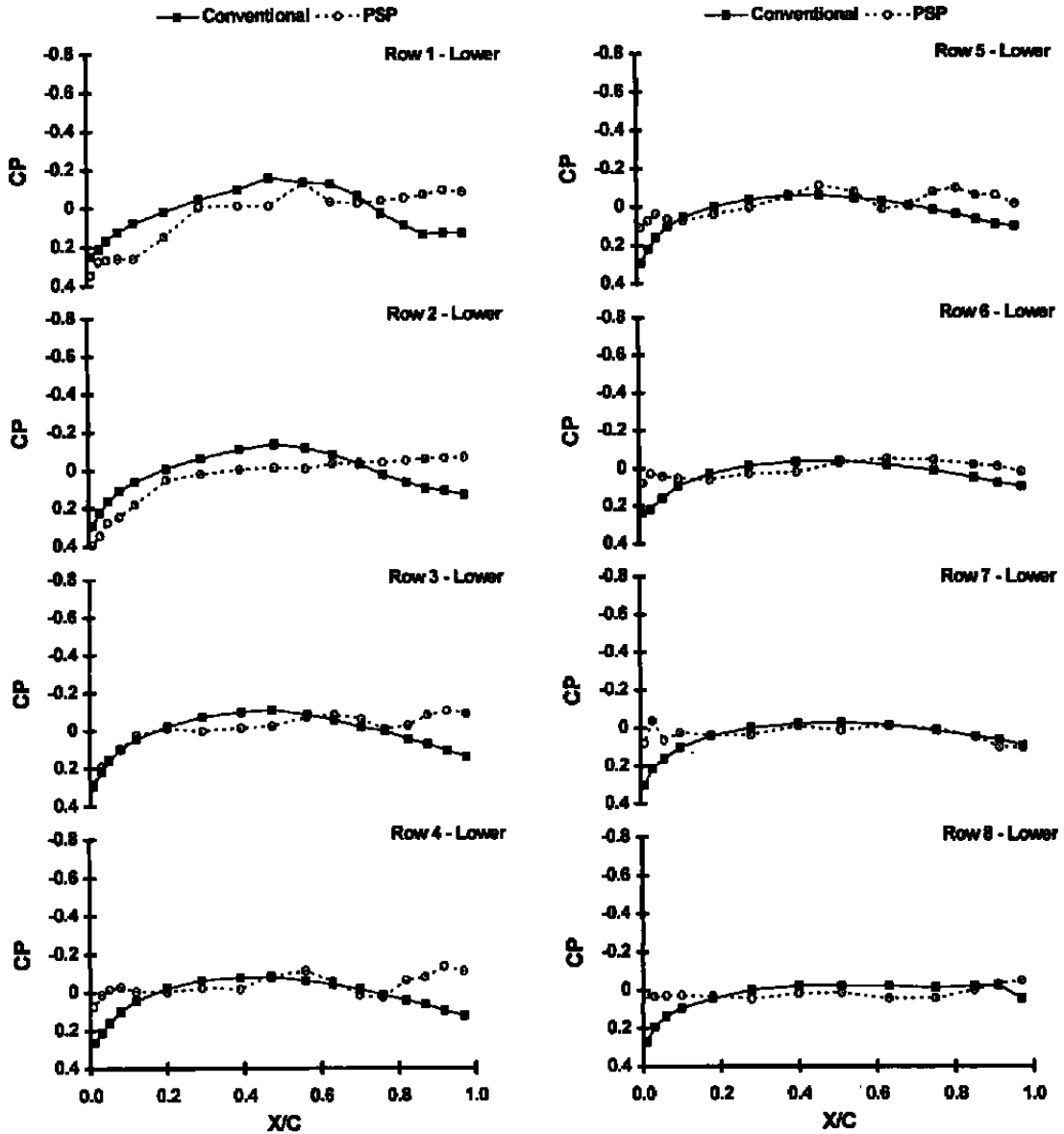
b. Horizontal tail lower surface, Mach = 0.6, Alpha = 6 deg

Figure 12. Continued.
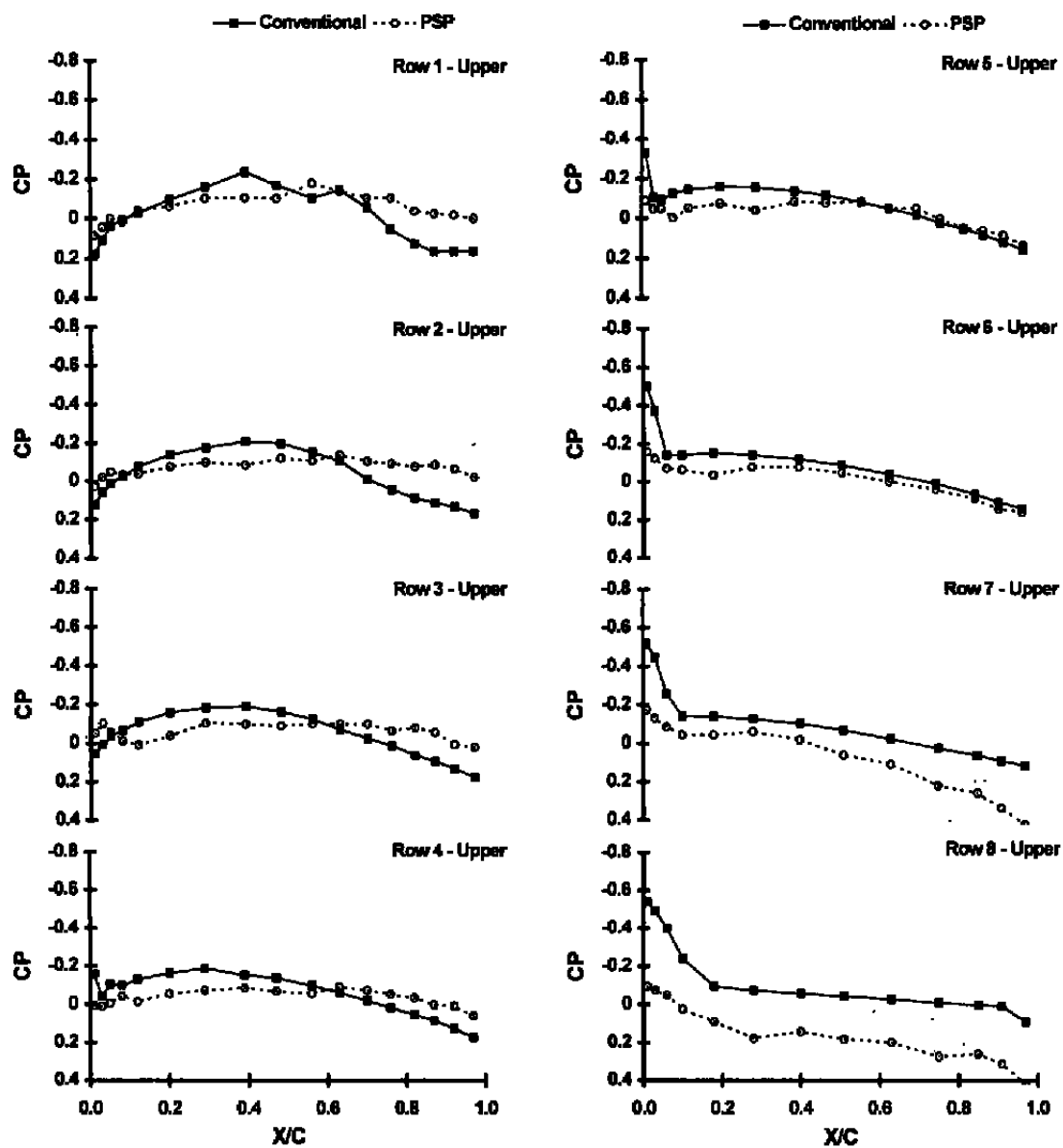
c. Horizontal tail upper surface, Mach = 0.85, Alpha = 6 deg
Figure 12. Continued.
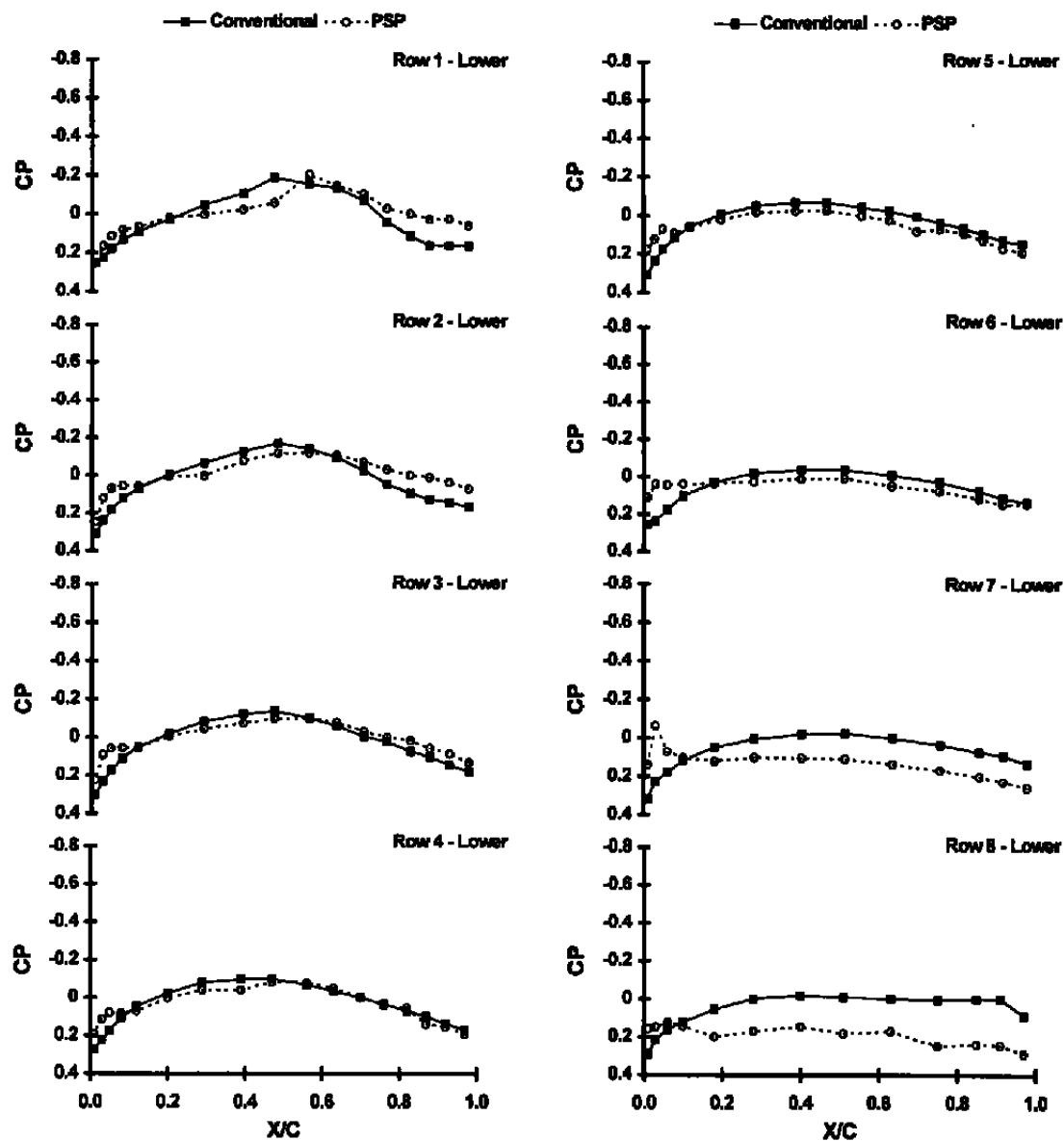
d. Horizontal tail lower surface, Mach = 0.85, Alpha = 6 deg

Figure 12. Continued.
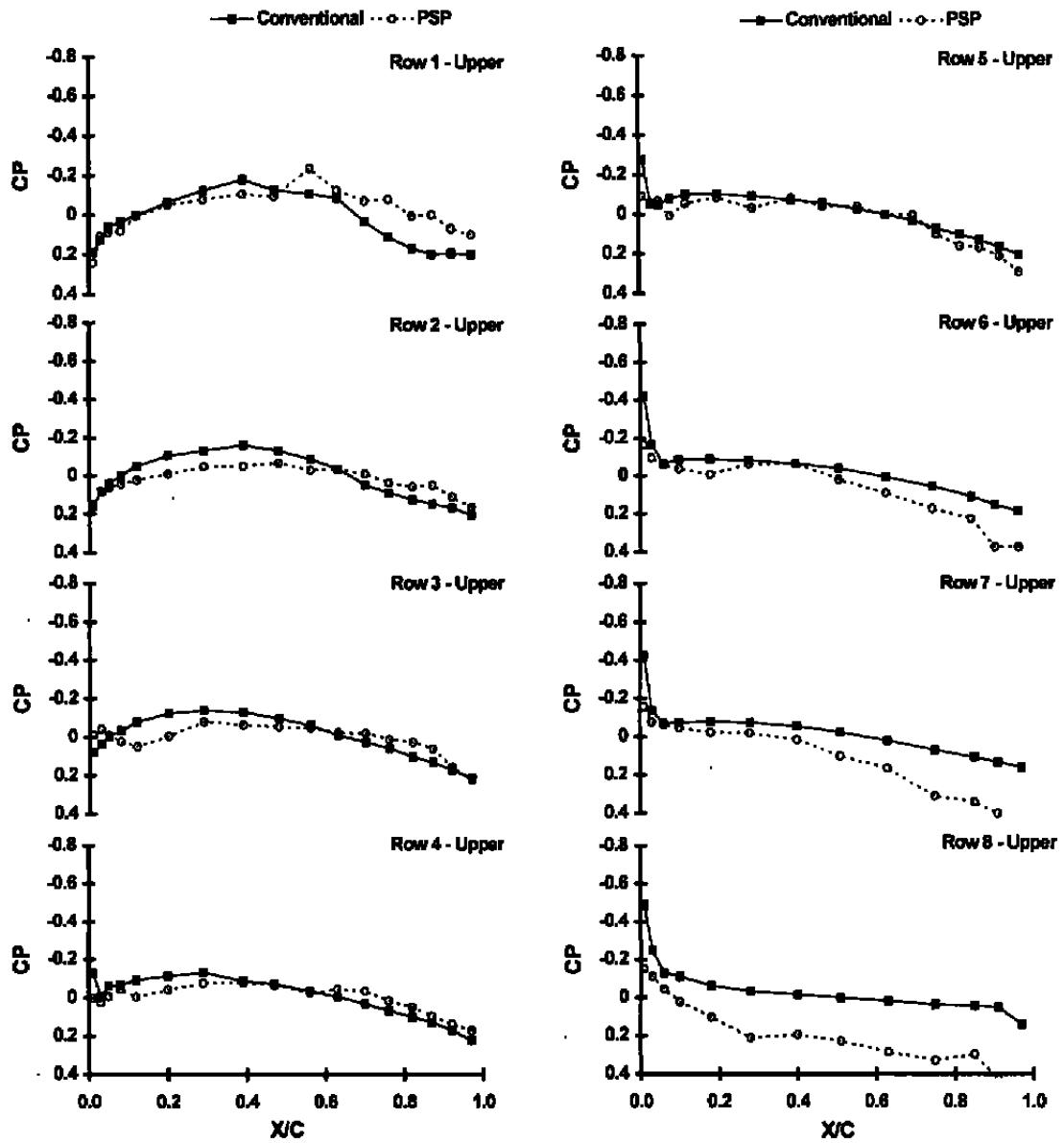
e. Horizontal tail upper surface, Mach = 0.95, Alpha = 6 deg

Figure 12. Continued.
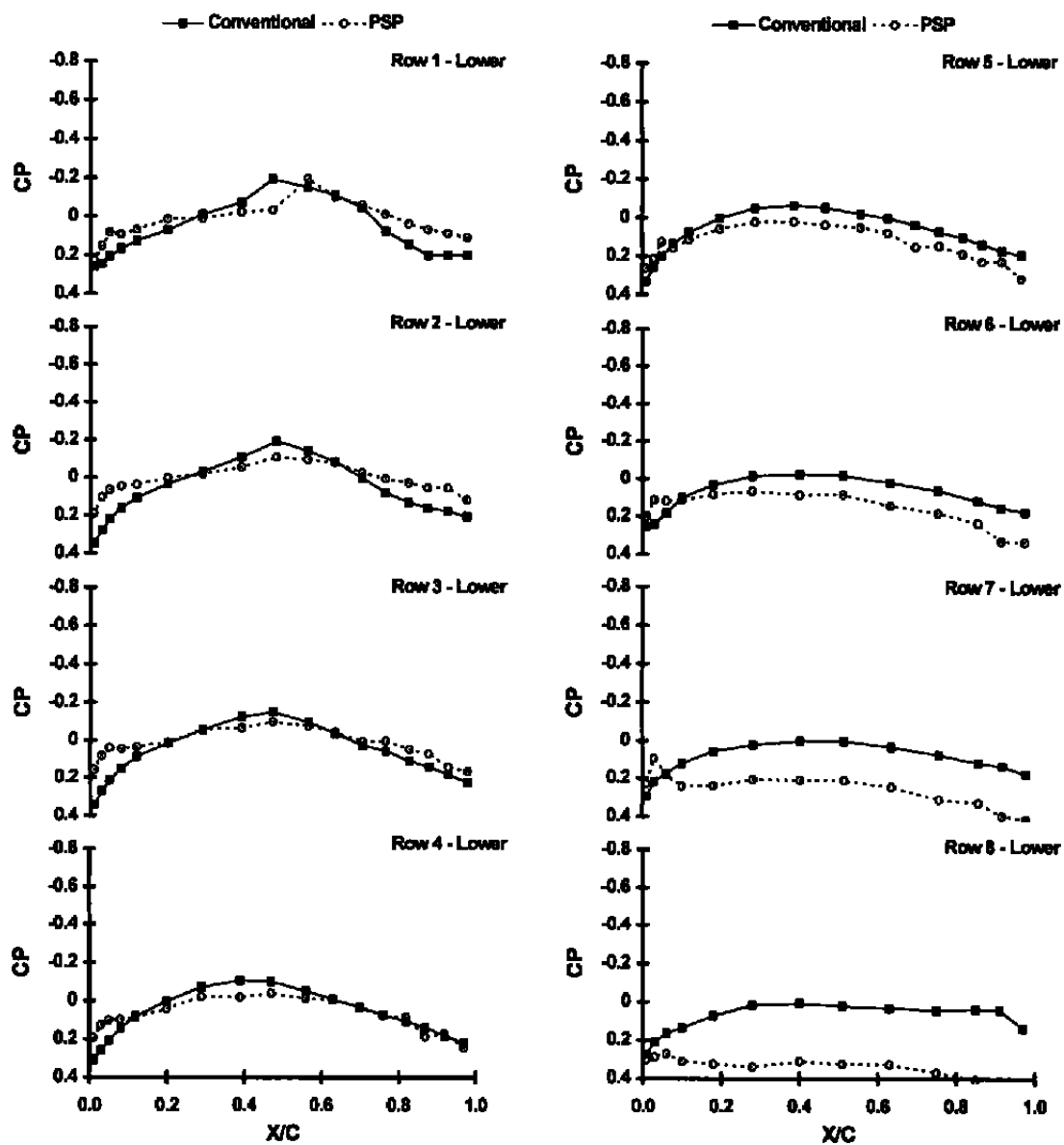
f. Horizontal tail lower surface, Mach = 0.95, Alpha = 6 deg

Figure 12. Continued.
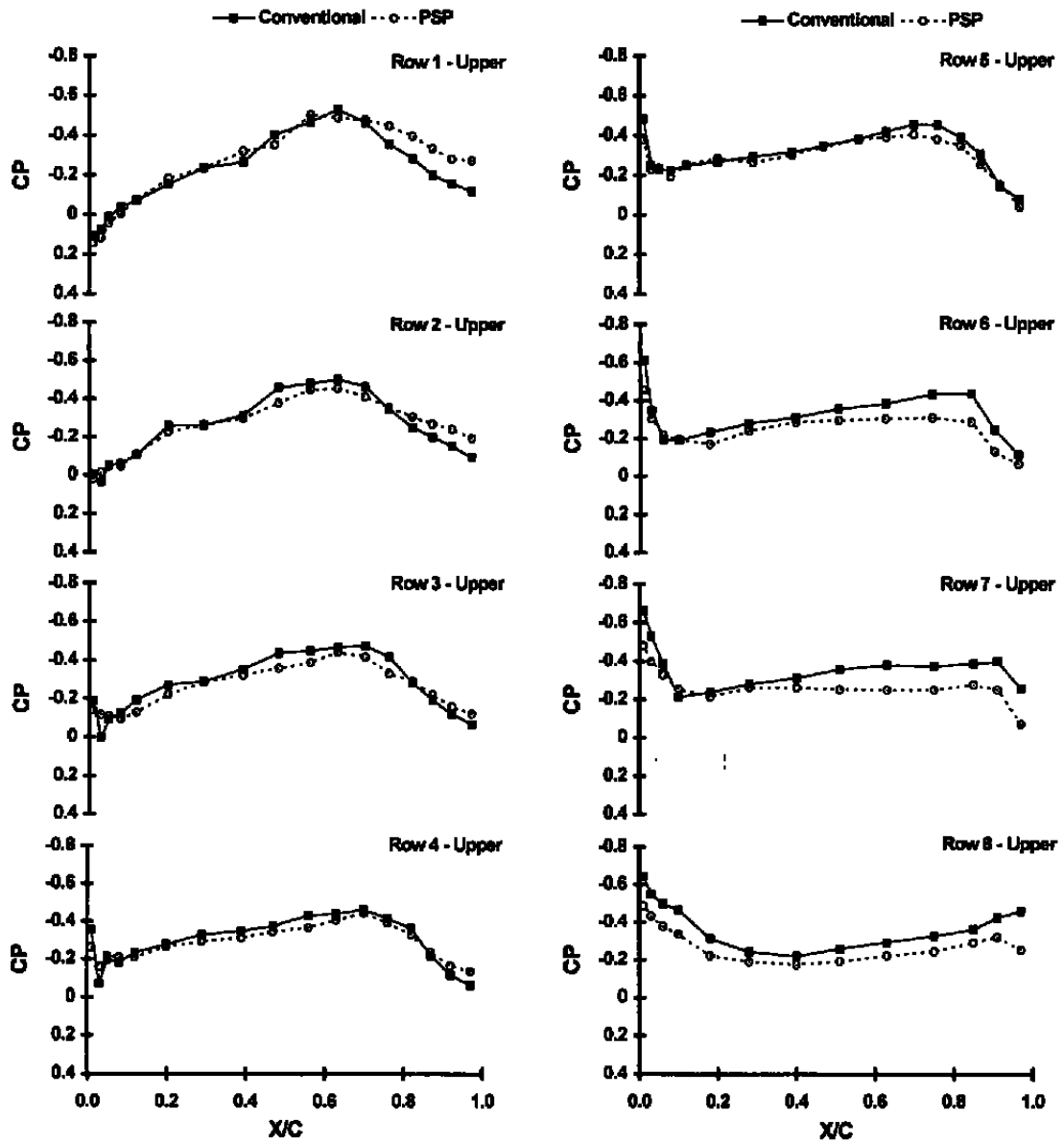
g. Horizontal tail upper surface, Mach = 1.2, Alpha = 6 deg
Figure 12. Continued.

41
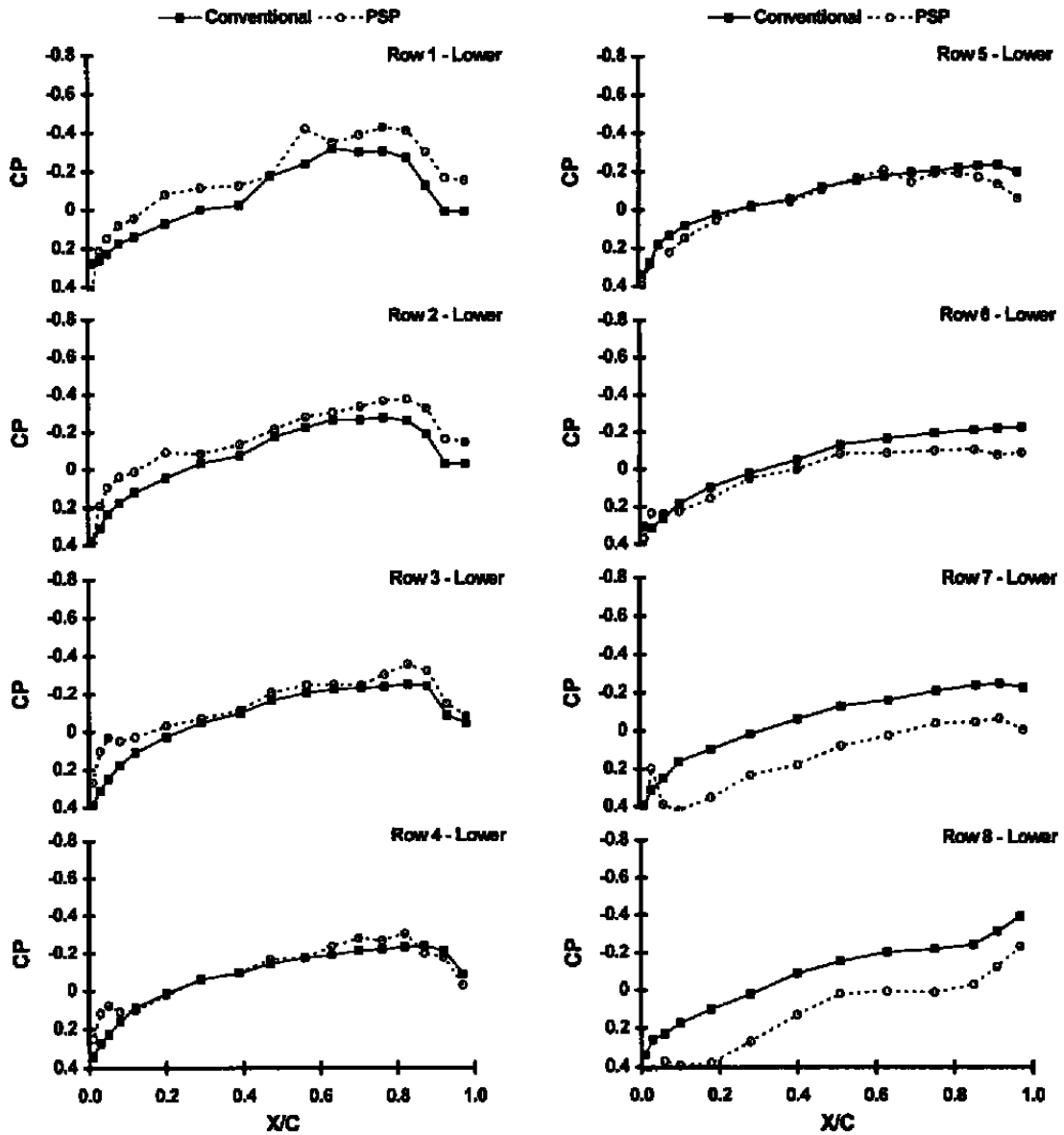
h. Horizontal tail lower surface, Mach = 1.2, Alpha = 6 deg
Figure 12. Concluded.
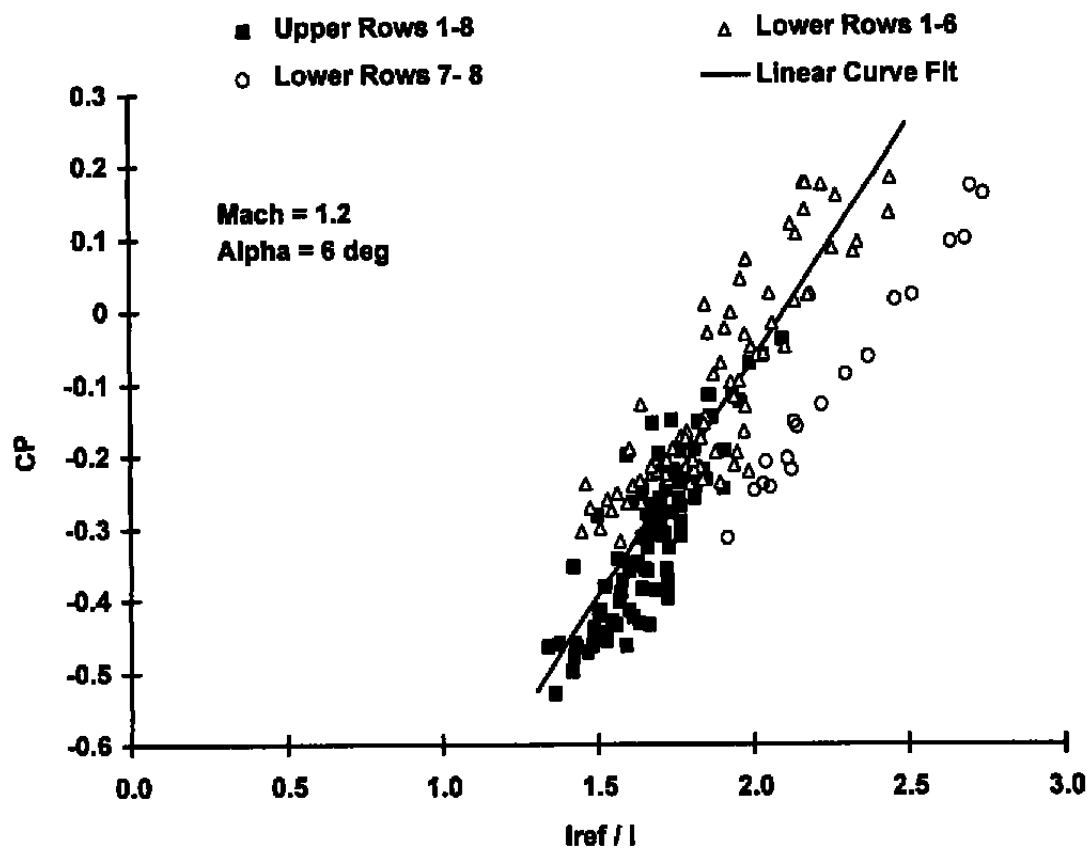
Figure 13. Sample of PSP curve-fit data.
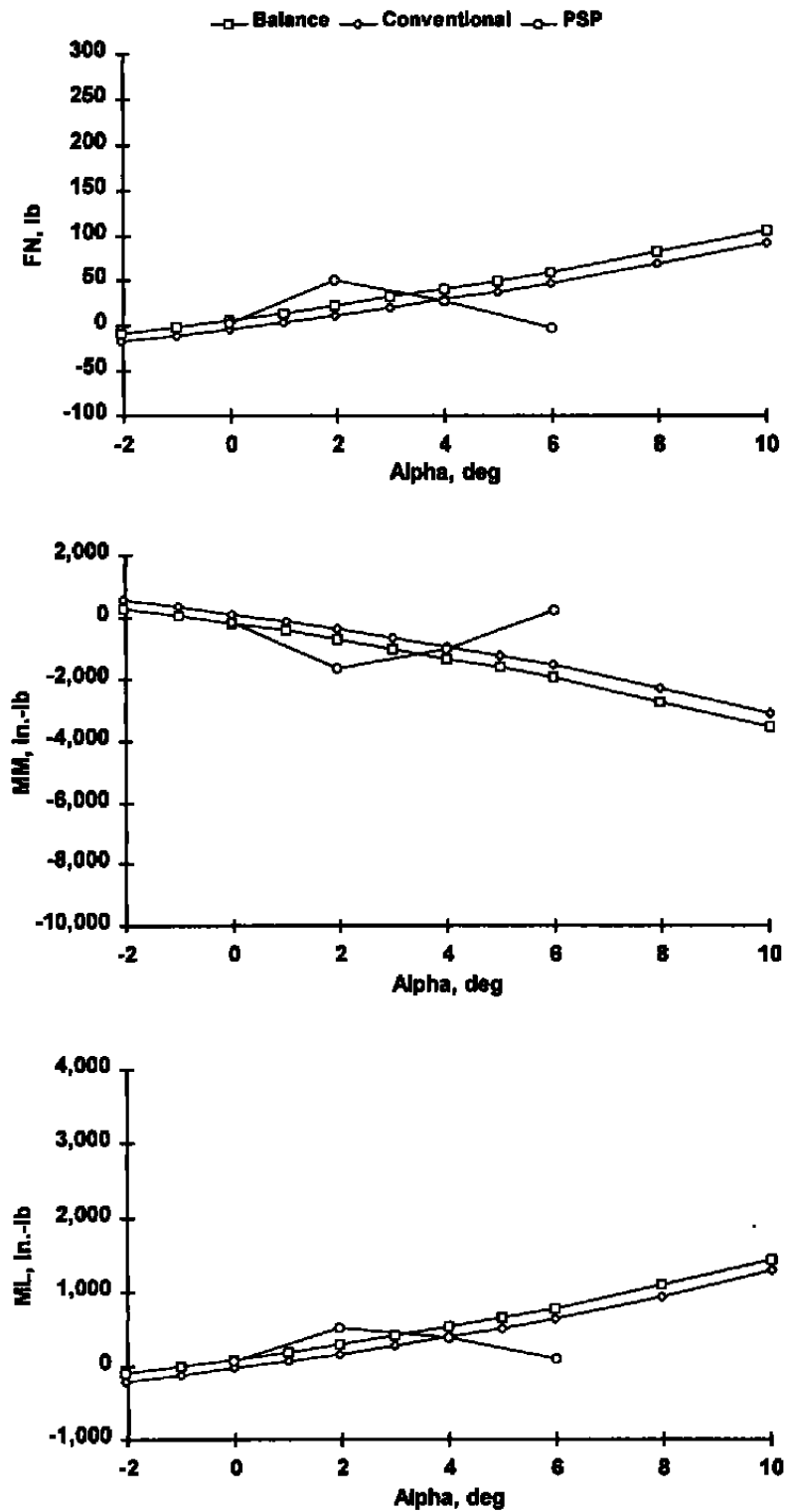
a. Mach = 0.6

Figure 14. F-18 E/F integrated loads comparison.
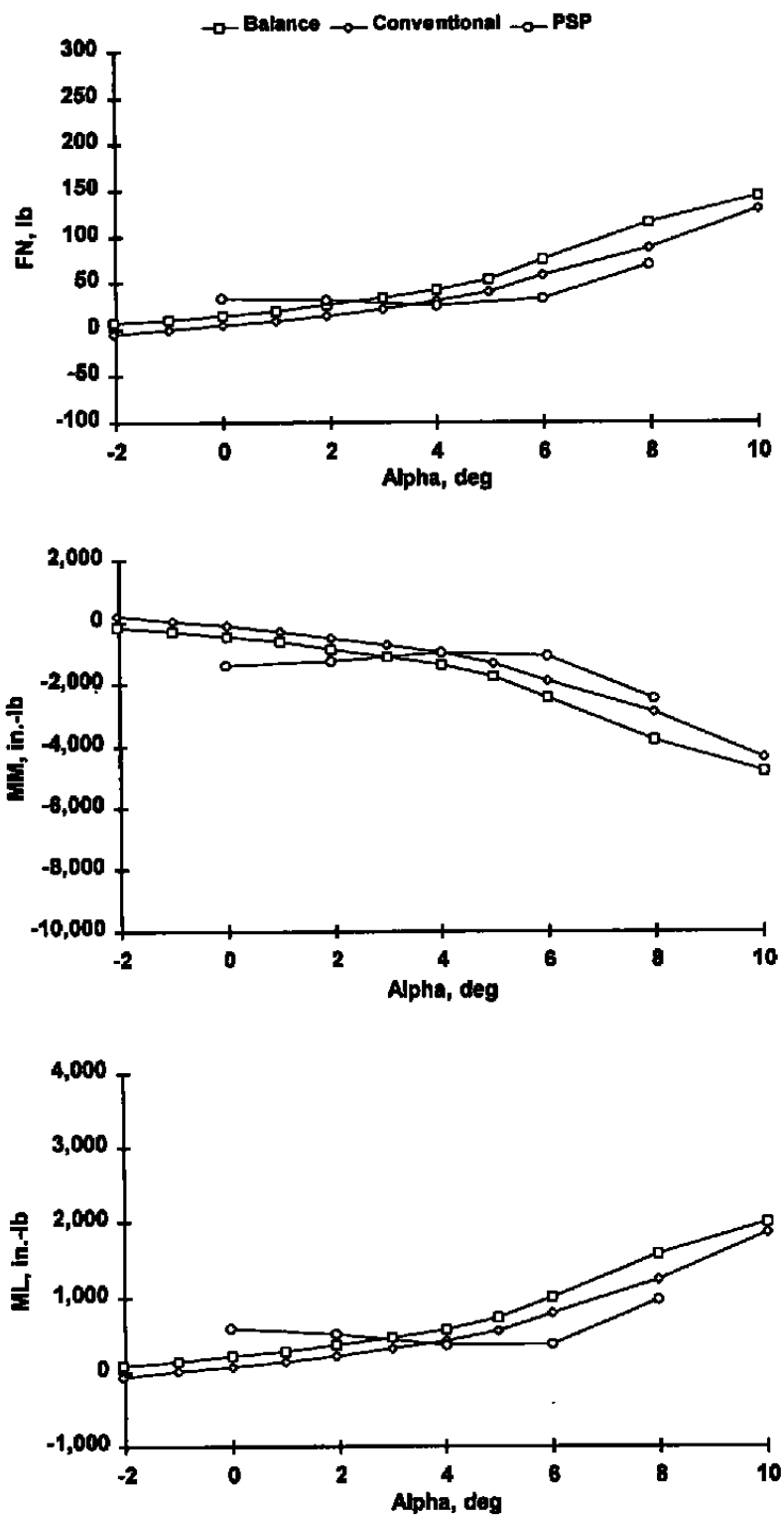
b. Mach = 0.85

Figure 14. Continued.

45
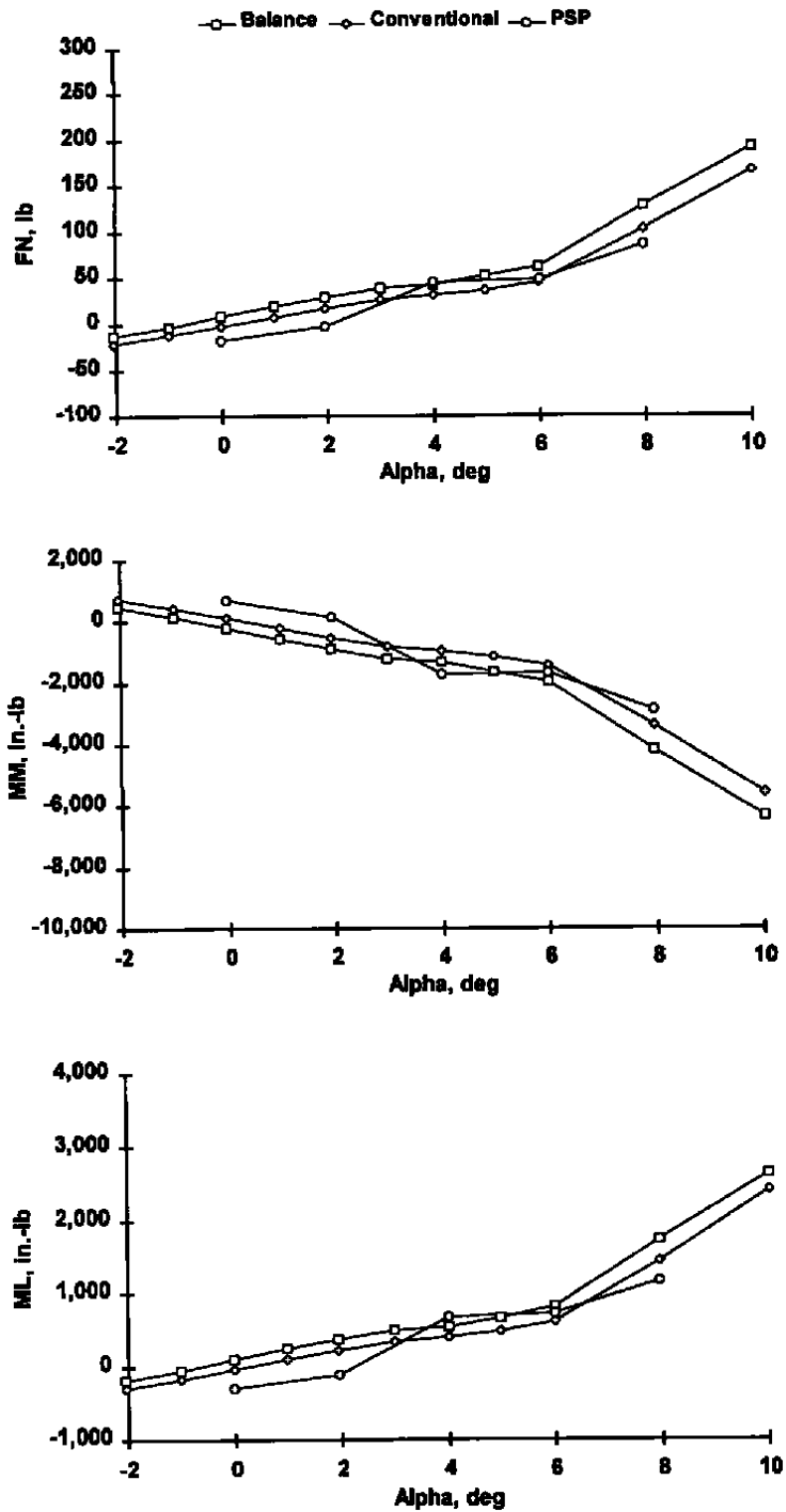
c. Mach = 0.95
Figure 14. Continued.
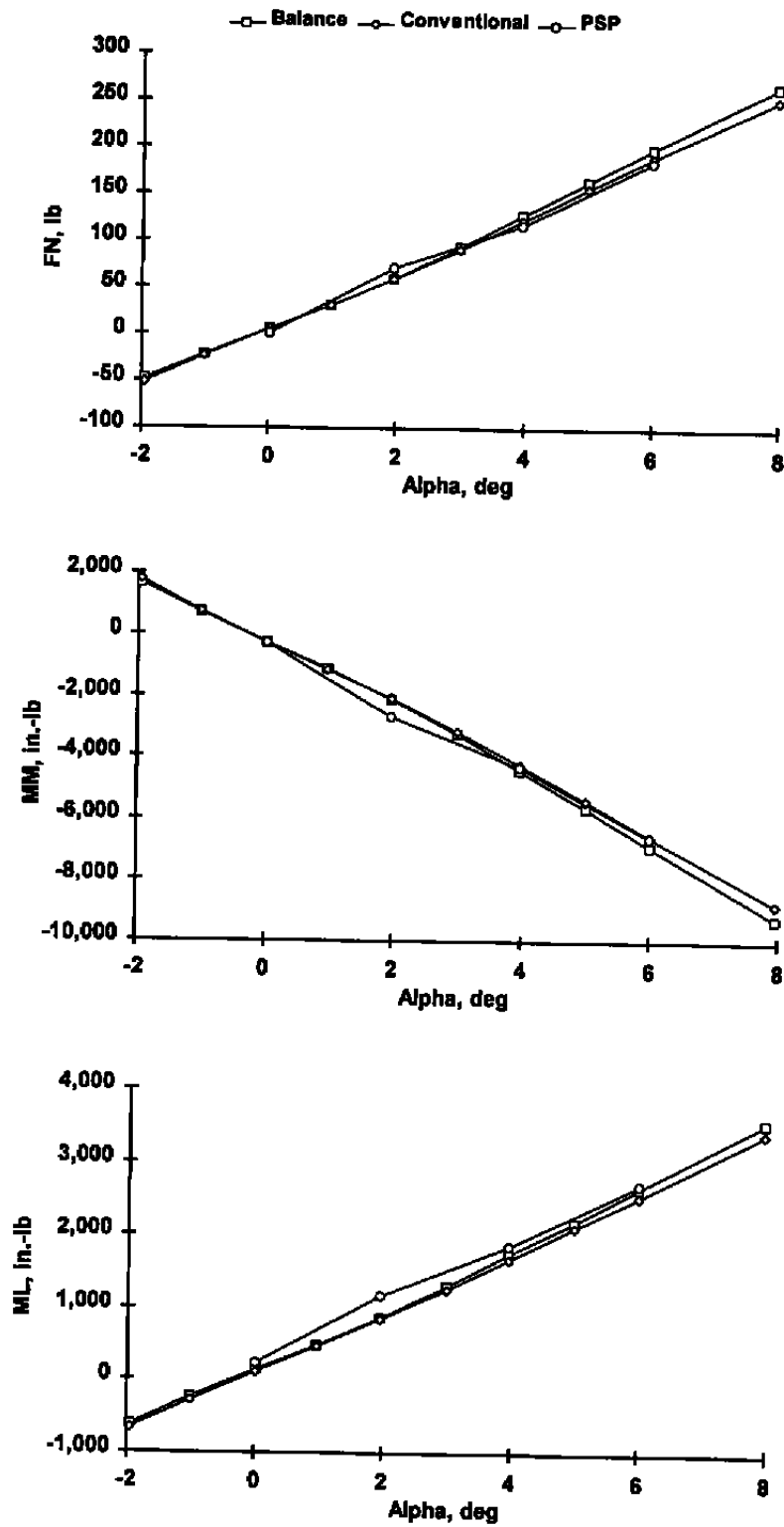
d. Mach = 1.2
Figure 14. Concluded.
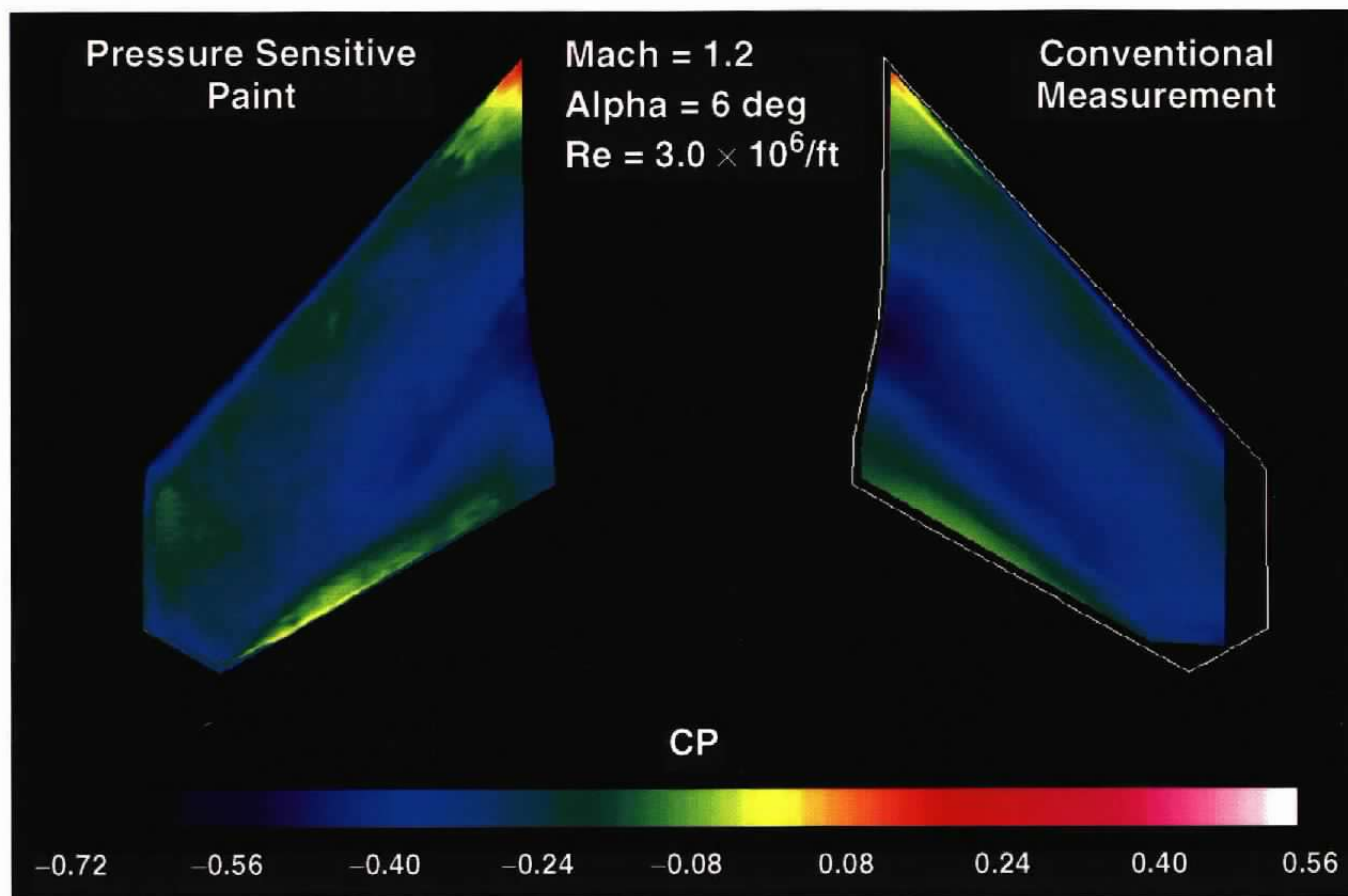
a. Upper surface, Mach = 1.2, Alpha = 6 deg

Figure 15. F-18 E/F pressure coefficient distribution comparison.
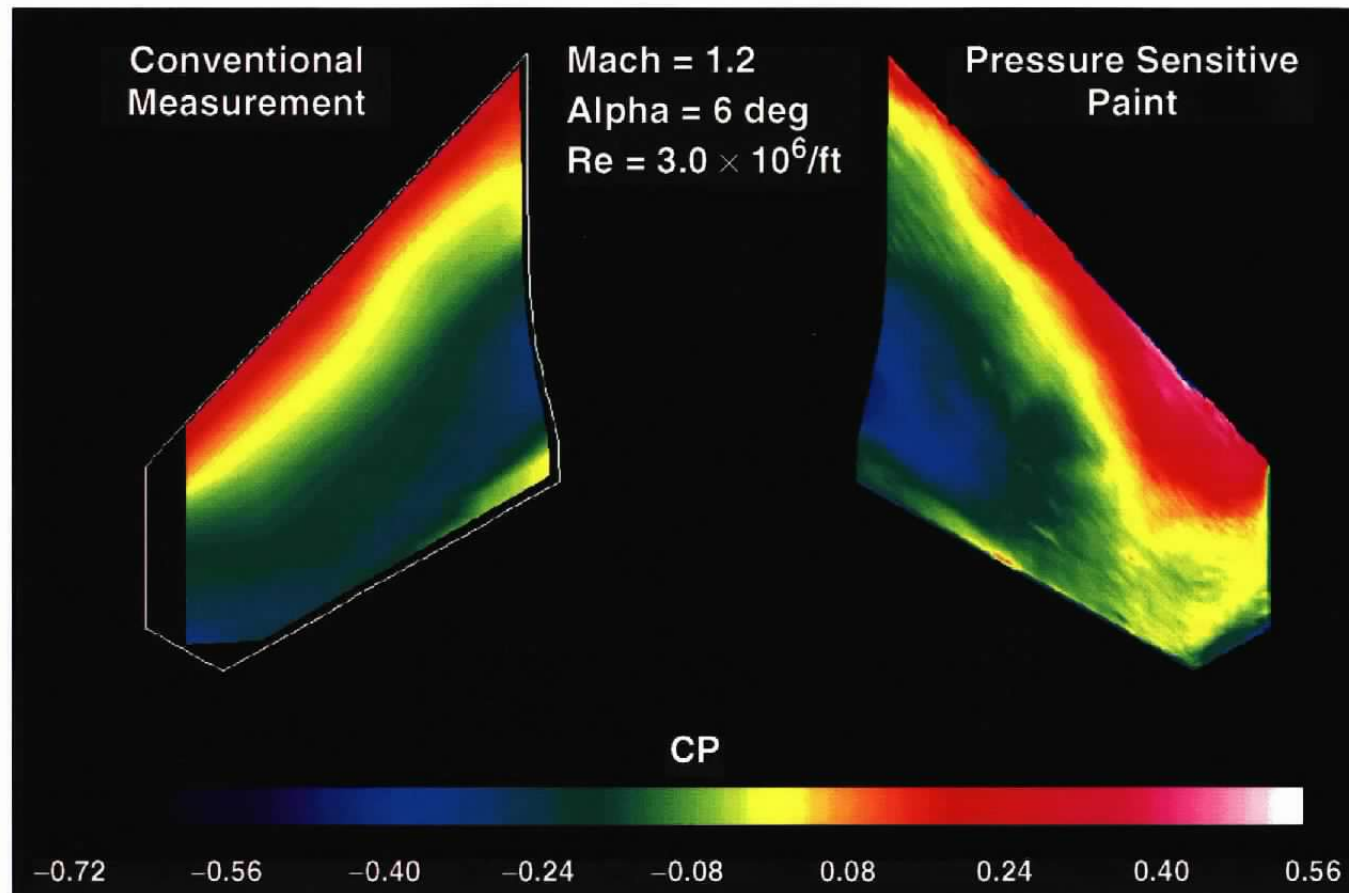
b. Lower surface, Mach = 1.2, Alpha = 6 deg
Figure 15. Concluded.

Table 1. TST Wing Pressure Orifice Designation and Location

Section & Tap No.	X/C	F.S.	B.L.	W.L.	Section & Tap No.	X/C	F.S.	B.L.	W.L.
101	1.000	32.157	2.515	2.907	201	1.000	32.411	3.894	2.846
102	0.960	31.706	2.527	3.023	202	0.960	32.020	3.904	2.940
103	0.920	31.234	2.535	3.106	203	0.920	31.582	3.911	3.013
104	0.870	30.657	2.546	3.205	204	0.870	31.142	3.919	3.086
105	0.810	29.964	2.558	3.323	205	0.810	30.557	3.929	3.181
106	0.740	29.156	2.572	3.455	206	0.740	29.874	3.940	3.285
107	0.670	28.348	2.585	3.580	207	0.670	29.191	3.950	3.379
108	0.600	27.540	2.598	3.700	208	0.600	28.508	3.959	3.466
109	0.530	26.732	2.610	3.815	209	0.530	27.826	3.967	3.546
110	0.460	25.924	2.622	3.924	210	0.460	27.143	3.975	3.617
111	0.390	25.117	2.631	4.015	211	0.390	26.459	3.981	3.673
112	0.320	24.309	2.638	4.081	212	0.320	25.777	3.984	3.710
113	0.250	23.500	2.642	4.117	213	0.250	25.094	3.986	3.723
114	0.180	22.693	2.642	4.117	214	0.180	24.411	3.984	3.707
115	0.130	22.115	2.639	4.091	215	0.130	23.923	3.981	3.674
116	0.090	21.654	2.634	4.041	216	0.090	23.533	3.976	3.625
117	0.060	21.307	2.626	3.969	217	0.060	23.240	3.969	3.559
118	0.040	21.077	2.618	3.887	218	0.040	23.045	3.961	3.489
119	0.020	20.846	2.604	3.759	219	0.020	22.850	3.950	3.384
120	0.008	20.707	2.591	3.631	220	0.008	22.733	3.940	3.285
121	0.000	20.615	2.568	3.416	221	0.000	22.655	3.922	3.118
122	0.008	20.707	2.550	3.239	222	0.008	22.733	3.907	2.974
123	0.020	20.846	2.542	3.168	223	0.020	22.850	3.901	2.916
124	0.050	21.192	2.530	3.057	224	0.050	23.143	3.891	2.824
125	0.100	21.769	2.517	2.930	225	0.100	23.631	3.881	2.722
126	0.180	22.693	2.502	2.789	226	0.180	24.411	3.869	2.613
127	0.280	23.847	2.491	2.680	227	0.280	25.387	3.861	2.536
128	0.380	25.001	2.486	2.631	228	0.380	26.362	3.858	2.509
129	0.490	26.270	2.487	2.644	229	0.490	27.435	3.861	2.538
130	0.600	27.541	2.494	2.715	230	0.600	28.508	3.870	2.617
131	0.700	28.694	2.504	2.803	231	0.700	29.484	3.879	2.709
132	0.790	29.733	2.512	2.880	232	0.790	30.362	3.888	2.792
133	0.870	30.657	2.516	2.922	233	0.870	31.142	3.893	2.841
134	0.940	31.465	2.515	2.913	234	0.940	31.746	3.893	2.844

Table 1. Continued

Section & Tap No.	X/C	F.S.	B.L.	W.L.	Section & Tap No.	X/C	F.S.	B.L.	W.L.
301	1.000	33.307	7.825	2.589	401	1.000	34.406	11.548	2.227
302	0.960	32.991	7.833	2.659	402	0.960	34.130	11.554	2.284
303	0.920	32.676	7.838	2.709	403	0.920	33.854	11.558	2.324
304	0.870	32.282	7.844	2.772	404	0.870	33.503	11.563	2.374
305	0.810	31.809	7.852	2.844	405	0.810	33.095	11.569	2.429
306	0.740	31.256	7.860	2.917	406	0.740	32.612	11.575	2.486
307	0.670	30.704	7.866	2.977	407	0.670	32.130	11.580	2.530
308	0.600	30.152	7.843	3.022	408	0.600	31.646	11.583	2.561
309	0.530	29.600	7.874	3.054	409	0.530	31.164	11.585	2.578
310	0.460	29.048	7.876	3.074	410	0.460	30.681	11.586	2.585
311	0.390	28.496	7.877	3.081	411	0.390	30.198	11.585	2.581
312	0.320	27.944	7.877	3.077	412	0.320	29.715	11.584	2.568
313	0.250	27.392	7.874	3.057	413	0.250	29.233	11.581	2.543
314	0.180	26.839	7.831	3.019	414	0.180	28.750	11.577	2.506
315	0.130	26.445	7.866	2.973	415	0.130	28.405	11.573	2.467
316	0.090	26.130	7.860	2.919	416	0.090	28.129	11.569	2.421
317	0.060	25.893	7.854	2.859	417	0.060	27.922	11.563	2.371
318	0.040	25.735	7.848	2.805	418	0.040	27.784	11.558	2.325
319	0.020	25.578	7.841	2.732	419	0.020	27.646	11.552	2.263
320	0.008	25.483	7.834	2.670	420	0.008	27.563	11.546	2.210
321	0.000	25.420	7.822	2.557	421	0.000	27.508	11.535	2.107
322	0.008	25.483	7.811	2.450	422	0.008	27.563	11.526	2.012
323	0.020	25.578	7.806	2.403	423	0.020	27.646	11.521	1.972
324	0.050	25.814	7.798	2.333	424	0.050	27.853	11.516	1.923
325	0.100	26.209	7.791	2.266	425	0.100	28.198	11.511	1.879
326	0.180	26.839	7.785	2.207	426	0.180	28.750	11.508	1.846
327	0.280	27.628	7.782	2.175	427	0.280	29.439	11.507	1.839
328	0.380	28.417	7.782	2.181	428	0.380	30.129	11.508	1.850
329	0.490	29.285	7.788	2.231	429	0.490	30.888	11.513	1.889
330	0.600	30.152	7.797	2.320	430	0.600	31.646	11.520	1.960
331	0.700	30.941	7.807	2.419	431	0.700	32.336	11.529	2.046
332	0.790	31.651	7.817	2.507	432	0.790	32.957	11.538	2.128
333	0.870	32.282	7.823	2.564	433	0.870	33.509	11.544	2.187
334	0.940	32.834	7.824	2.581	434	0.940	33.992	11.547	2.214

Table 1. Concluded

Section & Tap No.	X/C	F.S.	B.L.	W.L.
501	1.000	35.619	15.665	1.846
502	0.960	35.361	15.670	1.893
503	0.920	35.175	15.704	1.917
504	0.870	34.872	15.676	1.953
505	0.810	34.574	15.680	1.989
506	0.740	34.228	15.683	2.022
507	0.670	33.853	15.686	2.009
508	0.600	33.478	15.688	2.065
509	0.530	33.103	15.689	2.073
510	0.460	32.728	15.689	2.072
511	0.390	32.354	15.687	2.063
512	0.320	31.979	15.685	2.045
513	0.250	31.604	15.683	2.019
514	0.180	31.229	15.679	1.983
515	0.130	30.961	15.675	1.947
516	0.090	30.747	15.671	1.908
517	0.060	30.587	15.667	1.868
518	0.040	30.480	15.663	1.831
519	0.020	30.384	15.752	1.738
520	0.008	30.305	15.522	1.811
521	0.000	30.266	15.646	1.664
522	0.008	30.308	15.638	1.596
523	0.020	30.373	15.635	1.568
524	0.050	30.533	15.632	1.533
525	0.100	30.801	15.629	1.507
526	0.180	31.229	15.628	1.493
527	0.280	31.765	15.628	1.496
528	0.380	32.300	15.630	1.512
529	0.490	32.889	15.633	1.545
530	0.600	33.478	15.639	1.602
531	0.700	34.013	15.648	1.683
532	0.790	34.546	15.656	1.768
534	0.940	35.298	15.663	1.832

Table 2. F-18 E/F Horizontal Tail Pressure Orifice Designation and Location
a. Upper Surface

Tap No.	Percent Semispan	F.S.	B.L.	W.L.	Tap No.	Percent Semispan	F.S.	B.L.	W.L.
4001	0.04	110.070	5.984	14.959	4035	0.17	111.464	8.418	14.827
4002	0.04	109.269	5.981	15.035	4036	0.17	110.696	8.413	14.894
4003	0.04	108.455	6.027	15.109	4037	0.17	109.928	8.453	14.959
4004	0.04	107.622	6.205	15.180	4038	0.17	109.139	8.557	15.022
4005	0.04	106.734	6.400	15.250	4039	0.17	108.280	8.659	15.086
4006	0.04	105.741	6.606	15.318	4040	0.17	107.320	8.767	15.149
4007	0.04	104.632	6.799	15.376	4041	0.17	106.257	8.870	15.204
4008	0.04	103.405	6.926	15.419	4042	0.17	105.089	8.938	15.246
4009	0.04	102.080	6.993	15.441	4043	0.17	103.823	8.970	15.269
4010	0.04	100.663	7.029	15.429	4044	0.17	102.466	8.985	15.262
4011	0.04	99.165	7.054	15.378	4045	0.17	101.032	8.995	15.219
4012	0.04	97.604	7.075	15.275	4046	0.17	99.538	9.002	15.130
4013	0.04	96.414	7.088	15.156	4047	0.17	98.394	9.005	15.025
4014	0.04	95.697	7.095	15.067	4048	0.17	97.704	9.006	14.945
4015	0.04	95.219	7.099	15.000	4049	0.17	97.243	9.007	14.886
4016	0.04	94.900	7.102	14.952	4050	0.17	96.936	9.007	14.842
4017	0.04	94.589	7.106	14.900	4051	0.17	96.639	9.009	14.795
4018	0.10	110.659	7.018	14.904	4052	0.26	112.430	10.098	14.736
4019	0.10	109.874	7.011	14.975	4053	0.26	111.681	10.096	14.797
4020	0.10	109.087	7.071	15.045	4054	0.26	110.936	10.110	14.857
4021	0.10	108.282	7.230	15.112	4055	0.26	110.168	10.148	14.915
4022	0.10	107.407	7.386	15.179	4056	0.26	109.331	10.184	14.975
4023	0.10	106.429	7.551	15.245	4057	0.26	108.396	10.223	15.035
4024	0.10	105.343	7.708	15.300	4058	0.26	107.362	10.260	15.088
4025	0.10	104.146	7.816	15.342	4059	0.26	106.229	10.285	15.130
4026	0.10	102.845	7.862	15.365	4060	0.26	105.001	10.296	15.154
4027	0.10	101.451	7.885	15.356	4061	0.26	103.686	10.301	15.149
4028	0.10	99.978	7.900	15.308	4062	0.26	102.297	10.305	15.112
4029	0.10	98.443	7.912	15.212	4063	0.26	100.849	10.308	15.031
4030	0.10	97.270	7.917	15.100	4064	0.26	99.741	10.308	14.936
4031	0.10	96.563	7.919	15.014	4065	0.26	99.071	10.308	14.863
4032	0.10	96.091	7.921	14.951	4066	0.26	98.625	10.308	14.808
4033	0.10	95.777	7.922	14.904	4067	0.26	98.327	10.309	14.767
4034	0.10	95.471	7.925	14.854	4068	0.26	98.032	10.309	14.724

Table 2. Continued
a. Concluded

Tap No.	Percent Semispan	F.S.	B.L.	W.L.
4069	0.38	113.593	12.115	14.625
4070	0.38	112.882	12.115	14.679
4071	0.38	112.177	12.115	14.730
4072	0.38	111.451	12.115	14.782
4073	0.38	110.657	12.115	14.834
4074	0.38	109.772	12.115	14.888
4075	0.38	108.794	12.115	14.936
4076	0.38	107.722	12.115	14.974
4077	0.38	106.562	12.115	14.997
4078	0.38	105.319	12.115	14.994
4079	0.38	104.006	12.115	14.962
4080	0.38	102.639	12.115	14.892
4081	0.38	101.592	12.115	14.810
4082	0.38	100.957	12.115	14.747
4083	0.38	100.535	12.115	14.698
4084	0.38	100.254	12.115	14.663
4085	0.38	99.970	12.115	14.625
4086	0.53	114.794	14.283	14.510
4087	0.53	114.049	14.283	14.559
4088	0.53	113.174	14.283	14.615
4089	0.53	111.891	14.283	14.691
4090	0.53	110.367	14.283	14.762
4091	0.53	108.867	14.283	14.804
4092	0.53	107.367	14.283	14.808
4093	0.53	105.860	14.283	14.775
4094	0.53	104.463	14.283	14.705
4095	0.53	103.494	14.283	14.631
4096	0.53	102.965	14.283	14.581
4097	0.53	102.619	14.283	14.545
4098	0.53	102.320	14.283	14.509

Tap No.	Percent Semispan	F.S.	B.L.	W.L.
4099	0.70	116.270	16.832	14.369
4100	0.70	115.600	16.832	14.406
4101	0.70	114.814	16.832	14.447
4102	0.70	113.661	16.832	14.502
4103	0.70	112.292	16.832	14.555
4104	0.70	110.944	16.832	14.585
4105	0.70	109.597	16.832	14.588
4106	0.70	108.244	16.832	14.564
4107	0.70	106.988	16.832	14.512
4108	0.70	106.117	16.832	14.458
4109	0.70	105.641	16.832	14.422
4110	0.70	105.329	16.832	14.396
4111	0.70	105.060	16.832	14.370
4112	0.90	116.403	19.682	14.229
4113	0.90	115.904	19.684	14.268
4114	0.90	115.323	19.685	14.296
4115	0.90	114.469	19.685	14.323
4116	0.90	113.457	19.684	14.339
4117	0.90	112.462	19.688	14.343
4118	0.90	111.466	19.688	14.336
4119	0.90	110.464	19.683	14.317
4120	0.90	109.535	19.683	14.286
4121	0.90	108.889	19.682	14.257
4122	0.90	108.536	19.682	14.239
4123	0.90	108.305	19.682	14.226
4124	0.90	108.118	19.682	14.212

Table 2. Continued
b. Lower Surface

Tap No.	Percent Semispan	F.S.	B.L.	W.L.	Tap No.	Percent Semispan	F.S.	B.L.	W.L.
4201	0.04	110.064	5.980	14.870	4235	0.17	111.464	8.416	14.747
4202	0.04	109.266	5.975	14.795	4236	0.17	110.696	8.412	14.680
4203	0.04	108.450	6.016	14.716	4237	0.17	109.928	8.450	14.611
4204	0.04	107.618	6.186	14.627	4238	0.17	109.140	8.549	14.538
4205	0.04	106.729	6.374	14.536	4239	0.17	108.281	8.649	14.463
4206	0.04	105.737	6.569	14.448	4240	0.17	107.321	8.747	14.389
4207	0.04	104.632	6.744	14.372	4241	0.17	106.257	8.835	14.325
4208	0.04	103.408	6.861	14.316	4242	0.17	105.089	8.897	14.277
4209	0.04	102.079	6.933	14.286	4243	0.17	103.822	8.935	14.250
4210	0.04	100.660	6.974	14.295	4244	0.17	102.466	8.955	14.256
4211	0.04	99.163	7.003	14.343	4245	0.17	101.032	8.967	14.298
4212	0.04	97.603	7.034	14.443	4246	0.17	99.538	8.979	14.387
4213	0.04	96.411	7.061	14.560	4247	0.17	98.394	8.991	14.490
4214	0.04	95.693	7.078	14.649	4248	0.17	97.703	8.998	14.570
4215	0.04	95.215	7.089	14.715	4249	0.17	97.243	9.003	14.629
4216	0.04	94.896	7.096	14.763	4250	0.17	96.936	9.005	14.672
4217	0.04	94.588	7.103	14.813	4251	0.17	96.639	9.008	14.718
4218	0.10	110.660	7.015	14.818	4252	0.26	112.427	10.097	14.663
4219	0.10	109.875	7.010	14.746	4253	0.26	111.682	10.095	14.601
4220	0.10	109.088	7.068	14.671	4254	0.26	110.936	10.108	14.540
4221	0.10	108.284	7.220	14.588	4255	0.26	110.169	10.143	14.478
4222	0.10	107.409	7.372	14.504	4256	0.26	109.332	10.179	14.414
4223	0.10	106.430	7.524	14.422	4257	0.26	108.397	10.214	14.351
4224	0.10	105.342	7.658	14.351	4258	0.26	107.364	10.245	14.294
4225	0.10	104.144	7.755	14.299	4259	0.26	106.231	10.268	14.250
4226	0.10	102.844	7.812	14.270	4260	0.26	105.003	10.282	14.225
4227	0.10	101.450	7.842	14.278	4261	0.26	103.689	10.289	14.230
4228	0.10	99.978	7.860	14.323	4262	0.26	102.300	10.294	14.268
4229	0.10	98.443	7.879	14.418	4263	0.26	100.852	10.299	14.349
4230	0.10	97.270	7.897	14.530	4264	0.26	99.743	10.304	14.444
4231	0.10	96.562	7.908	14.615	4265	0.26	99.073	10.306	14.517
4232	0.10	96.091	7.915	14.678	4266	0.26	98.626	10.308	14.571
4233	0.10	95.776	7.920	14.724	4267	0.26	98.328	10.308	14.611
4234	0.10	95.471	7.923	14.772	4268	0.26	98.026	10.309	14.652

Table 2. Concluded
b. Concluded

Tap No.	Percent Semispan	F.S.	B.L.	W.L.
4269	0.38	113.588	12.114	14.561
4270	0.38	112.883	12.114	14.508
4271	0.38	112.178	12.113	14.457
4272	0.38	111.451	12.113	14.405
4273	0.38	110.658	12.113	14.353
4274	0.38	109.774	12.112	14.299
4275	0.38	108.796	12.113	14.252
4276	0.38	107.725	12.113	14.214
4277	0.38	106.565	12.114	14.192
4278	0.38	105.323	12.115	14.195
4279	0.38	104.011	12.116	14.228
4280	0.38	102.642	12.117	14.298
4281	0.38	101.594	12.117	14.380
4282	0.38	100.960	12.117	14.443
4283	0.38	100.537	12.116	14.491
4284	0.38	100.255	12.116	14.525
4285	0.38	99.970	12.115	14.562
4286	0.53	114.792	14.283	14.450
4287	0.53	114.049	14.282	14.400
4288	0.53	113.175	14.282	14.345
4289	0.53	111.893	14.282	14.269
4290	0.53	110.370	14.282	14.198
4291	0.53	108.870	14.282	14.157
4292	0.53	107.370	14.283	14.153
4293	0.53	105.863	14.283	14.186
4294	0.53	104.465	14.284	14.257
4295	0.53	103.496	14.284	14.330
4296	0.53	102.966	14.284	14.380
4297	0.53	102.620	14.283	14.417
4298	0.53	102.320	14.283	14.450
4299	0.70	116.271	16.832	14.323
4300	0.70	115.600	16.832	14.287
4301	0.70	114.815	16.832	14.246
4302	0.70	113.662	16.832	14.191
4303	0.70	112.293	16.832	14.138
4304	0.70	110.946	16.832	14.108
4305	0.70	109.599	16.832	14.105
4306	0.70	108.245	16.832	14.130
4307	0.70	106.989	16.832	14.182
4308	0.70	106.118	16.832	14.235
4309	0.70	105.641	16.832	14.271
4310	0.70	105.329	16.832	14.298
4311	0.70	105.060	16.832	14.322
4312	0.90	116.404	19.680	14.165
4313	0.90	115.906	19.679	14.126
4314	0.90	115.325	19.678	14.098
4315	0.90	114.471	19.678	14.071
4316	0.90	113.457	19.678	14.056
4317	0.90	112.460	19.679	14.051
4318	0.90	111.464	19.679	14.058
4319	0.90	110.462	19.679	14.077
4320	0.90	109.533	19.680	14.108
4321	0.90	108.888	19.680	14.137
4322	0.90	108.535	19.681	14.155
4323	0.90	108.304	19.681	14.169
4324	0.90	108.118	19.681	14.182

Table 3. PSP Curve-Fit Coefficients
a. TST Test

Mach Number	Dynamic Pressure, psf	Static Pressure, psfa	Alpha, deg	A, psfa	B, psf
0.600	290	1,151	0	725.9	179.8
			2	602.9	226.5
			4	556.8	239.5
			6	402.8	304.2
0.600	290	1,151	8	357.9	318.1
0.835	374	764	0	-98.8	534.8
			2	-183.0	570.7
			4	-267.9	679.6
			6	-235.3	613.4
0.835	374	764	8	-185.2	590.2
0.900	392	692	0	-192.4	647.6
			2	-183.3	616.2
			4	-182.6	613.9
			6	-235.1	655.4
0.900	392	692	8	-217.8	647.6

Table 3. Concluded
b. F-18 E/F Test

Mach Number	Dynamic Pressure, psf	Static Pressure, psfa	Alpha, deg	Upper Surface		Lower Surface	
				A, psfa	B, psf	A, psfa	B, psf
0.60	379	1,503	0	1,127.6	139.8	1,162.7	79.6
			2	1,206.5	103.9	1,118.3	95.8
↓	↓	↓	4	1,355.0	49.3	1,288.7	50.2
0.60	379	1,503	6	977.5	196.1	1,145.5	85.0
0.85	498	986	0	694.8	115.0	496.7	151.0
			2	504.7	197.0	491.6	151.5
			4	517.7	196.7	546.4	136.6
↓	↓	↓	6	472.9	221.1	426.0	181.1
0.85	498	986	8	370.7	257.4	543.2	150.0
0.95	537	851	0	326.5	249.1	405.3	164.2
			2	296.0	262.8	350.2	181.4
			4	352.6	229.9	307.8	200.5
↓	↓	↓	6	137.3	322.1	322.6	199.0
0.95	537	851	8	65.1	343.5	427.4	163.5
1.20	612	607	0	-108.0	333.6	- - - -	- - - -
			2	-149.0	357.3	- - - -	- - - -
↓	↓	↓	4	-173.3	371.4	- - - -	- - - -
1.20	612	607	6	-236.4	400.6	- - - -	- - - -

NOMENCLATURE

A   Intercept of paint luminescence calibration, psfa [see Eq. (3)]

Alpha   Model angle of attack, deg

B   Sensitivity of paint luminescence calibration, psf [see eq. (3)]

B.L.   Model buttock line, in.

CP   Surface pressure coefficient

FN   Normal force, lb

F.S.   Model fuselage station, in.

I Paint luminscence intensity at pressure, wind-on condition

I_0 Paint luminescence intensity in the absence of oxygen

I_{ref} Paint luminescence intensity at reference pressure, wind-off condition

K_q Stern-Volmer constant

Mach   Free-stream Mach number

ML   Rolling (hinge) moment, in-lb

MM   Pitching moment, in.-lb

P Pressure at wind-on condition, psfa

P_{O2} Partial pressure of oxygen, psfa

P_{ref} Pressure at wind-off condition, psfa

Re   Free-stream unit Reynolds number, per foot

W. L.   Model water line, in.

X/C   Ratio of pressure orifice position (as measured from wing leading edge) to local chord